Phylogenetic relationships of Microdontinae (Diptera: Syrphidae) based on molecular and morphological characters

Reemer, Menno

2013-10

Reemer , M & Ståhls , G 2013 , ' Phylogenetic relationships of Microdontinae (Diptera: Syrphidae) based on molecular and morphological characters ' , Systematic Entomology , vol. 38 , no. 4 , pp. 661-688 . https://doi.org/10.1111/syen.12020

http://hdl.handle.net/10138/232626
https://doi.org/10.1111/syen.12020

Systematic Entomology

Systematic Entomology (2013), **38**, 661–688 DOI: 10.1111/syen.12020

Phylogenetic relationships of Microdontinae (Diptera: Syrphidae) based on molecular and morphological characters

MENNO REEMER[1] and GUNILLA STÅHLS[2]

[1]Naturalis Biodiversity Center, European Invertebrate Survey, Leiden, The Netherlands and [2]Finnish Museum of Natural History, University of Helsinki, Helsinki, Finland

Abstract. The intrasubfamilial classification of Microdontinae Rondani (Diptera: Syrphidae) has been a challenge: until recently more than 300 out of more than 400 valid species names were classified in *Microdon* Meigen. We present phylogenetic analyses of molecular and morphological characters (both separate and combined) of Microdontinae. The morphological dataset contains 174 characters, scored for 189 taxa (9 outgroup), representing all 43 presently recognized genera and several subgenera and species groups. The molecular dataset, representing 90 ingroup species of 28 genera, comprises sequences of five partitions in total from the mitochondrial gene *COI* and the nuclear ribosomal genes *18S* and *28S*. We test the sister-group relationship of *Spheginobaccha* with the other Microdontinae, attempt to elucidate phylogenetic relationships within the Microdontinae and discuss uncertainties in the classification of Microdontinae. Trees based on molecular characters alone are poorly resolved, but combined data are better resolved. Support for many deeper nodes is low, and placement of such nodes differs between parsimony and Bayesian analyses. However, *Spheginobaccha* is recovered as highly supported sister group in both. Both analyses agree on the early branching of *Mixogaster*, *Schizoceratomyia*, *Afromicrodon* and *Paramicrodon*. The taxonomical rank in relation to the other Syrphidae is discussed briefly. An additional analysis based on morphological characters only, including all 189 taxa, used implied weighting. A range of weighting strengths (k-values) is applied, chosen such that values of character fit of the resulting trees are divided into regular intervals. Results of this analysis are used for discussing the phylogenetic relationships of genera unrepresented in the molecular dataset.

Introduction

The Microdontinae, a subfamily of Syrphidae (Diptera), are distributed over all continents except Antarctica. The vast majority of the 454 described species occurs in the tropics, of which 203 are in the Neotropics. With 64 species known from the Holarctic region, the group is less well represented in temperate regions (Reemer & Ståhls, 2013), perhaps explaining the limited taxonomic attention.

Correspondence: Menno Reemer, Naturalis Biodiversity Center, European Invertebrate Survey, PO Box 9517, 2300 RA Leiden, The Netherlands. E-mail:menno.reemer@naturalis.nl

Since Rondani (1845) introduced the family group name Microdonellae, this group has been recognized as distinct from other Syrphidae, albeit under different spellings and taxonomic ranks. Only occasionally genera were included which nowadays are considered to belong elsewhere (Lioy, 1864; Williston, 1886; Shatalkin, 1975a,b). However, placement of the group relative to other Syrphidae has been unstable, with treatment as a tribe within the subfamily Syrphinae (Williston, 1886), a subtribe within the tribe Volucellini (Goffe, 1952), a family (Thompson, 1972) and a subfamily (Verrall, 1901; Ståhls *et al.*, 2003; Cheng & Thompson, 2008) (see Reemer & Ståhls, 2013).

The most recent advocates of a family status for Microdontinae are Thompson (1972) and Speight (1987, 2010), based on

the 'basal' relationship of Microdontinae with other Syrphidae as inferred by Thompson (1969) from a Hennigian argumentation scheme of characters considered of critical importance. Speight (1987) found additional morphological differences between Microdontinae and other Syrphidae used to support family status. Recent studies have confirmed this sister-group relationship (Skevington & Yeates, 2000; Ståhls *et al.*, 2003; Rotheray & Gilbert, 2008). Although most recent authors consider the group as a subfamily of the Syrphidae (Ståhls *et al.*, 2003; Cheng & Thompson, 2008), others prefer family rank (Speight, 2010).

Classification of *Spheginobaccha* de Meijere has received special attention by several authors and its phylogenetic position has shifted between different subfamilies of Syrphidae (reviewed by Thompson, 1974). The first to include this genus in the Microdontinae was Hull (1949), after which Thompson (1969) excluded it, but Shatalkin (1975a) included it again. Based on a phylogenetic analysis of combined morphological and molecular data, Ståhls *et al.* (2003) placed *Spheginobaccha* in the Microdontinae with the genus assigned as the sister group to all other Microdontinae.

Previous phylogenetic hypotheses concerning Microdontinae relied on too few taxa in relation to the high morphological diversity, for example, two in Skevington & Yeates (2000) and six in Ståhls *et al.* (2003) and Hippa & Ståhls (2005). Relationships within the Microdontinae remain completely unaddressed. Specifically, the supposed sister-group relationship of *Spheginobaccha* and the other Microdontinae needs testing by much broader taxon sampling. For instance, *Aristosyrphus* Curran, *Eurypterosyrphus* Barretto & Lane and *Mixogaster* Macquart share features with *Spheginobaccha*, such as a hypandrium with apical part consisting of two separate lobes, an unfurcate phallus and characters of wing venation (Reemer & Ståhls, 2013). An extended taxon set maximally representing genus groups (whether recognized previously or not) better tests this sister-group relationship.

Here we examine the phylogenetic relationships of the (sub)genera within the subfamily, based on molecular and morphological characters. We analyse a combination of morphological and molecular characters from a large set of microdontine taxa to test the sister-group relationship of *Spheginobaccha* with the other Microdontinae, attempt to elucidate phylogenetic relationships within the Microdontinae and discuss uncertainties in the classification of Microdontinae as proposed by Reemer & Ståhls (2013). The rank of the group in relation to the other Syrphidae is discussed briefly.

Materials and methods

Selection of ingroup taxa and specimens

The starting point for the selection of ingroup taxa for morphological analysis were the genus group names of Microdontinae listed by Cheng & Thompson (2008), and further revised by Reemer & Ståhls (2013). At least one species, preferably the type species, of all groups was included in the morphological dataset. Exceptions are objective or otherwise obvious synonyms (e.g. *Aphritis* Macquart, *Colacis* Gistel, *Holmbergia* Lynch Arribalzaga) and taxa based only on immature stages (e.g. *Ceratoconcha* Simroth, *Nothomicrodon* Wheeler) (for more information on these names and synonymies, see Cheng & Thompson, 2008). Many new or little known species were included which had been unassigned previously, or were lumped under *Microdon* despite morphological peculiarities. Descriptions can be found in Reemer & Ståhls (2013). When possible, more than one species per genus group was included: for *Spheginobaccha* the six species represent all three species groups of Thompson (1974).

The studied specimens were obtained from many sources. When possible, the primary types were studied, especially when no additional material was available. All specimens used for constructing the morphological matrix are listed in Table S1.

Characters were scored mostly from males. For four taxa of which only females were available, male genital characters were derived from closely related species. This approach was implemented only for taxa closely similar in external morphology, and which obviously belong to the same genus or species group (indicated in the 'remarks' column in Table S1).

In the molecular dataset, as many taxa as possible were included, depending on the availability of specimens for molecular analyses. The list of specimens used for DNA extraction, including locality and collection data as well as GenBank accession numbers, is given in Table S1. Morphological and molecular characters are based on specimens of the same species, except for *Rhopalosyrphus ramulorum* Weems & Deyrup for which morphological characters are based on a specimen of the closely related *R. guntheri* (Lynch Arribalzaga).

Specimens used for DNA extraction came from a wide variety of sources and collection methods. Fresh material (up to 3 years old) collected directly into ethanol was rare, so older material (up to about 10 years old), sometimes preserved dry, was used also. PCR results thus differed strongly among the taxa and among the genetic markers.

Root and outgroup

The analysis was rooted on *Chalarus spurius* (Fallén) (Diptera: Pipunculidae). Pipunculidae have been previously recovered as the sister group of Syrphidae (Skevington & Yeates, 2000; Yeates *et al.*, 2007; Rotheray & Gilbert, 2008). *Chalarus* Walker is a presumed 'basal' taxon in the pipunculid phylogeny (Rafael & De Meyer, 1992; Skevington & Yeates, 2000). The outgroup includes another pipunculid, *Nephrocerus lapponicus* Zetterstedt as well as selected taxa from the syrphid subfamilies Syrphinae and Eristalinae, which together form the putative sister of Microdontinae (Ståhls *et al.*, 2003; Hippa & Ståhls, 2005). Taxa were selected from tribes Chrysogasterini [*Neoascia tenur* (Harris), Eristalini *Eristalis tenax* (Linnaeus), Merodontini *Merodon equestris* (Fabricius), Pipizini *Pipiza noctiluca* (Linnaeus), Syrphini *Melanostoma scalare* (Fabricius), *Syrphus vitripennis* Meigen, Xylotini *Xylota segnis* (Linnaeus)].

Terminology

Our morphological terminology derives from McAlpine (1981), specifically as applied to Syrphidae by Thompson (1999), who introduced several new terms. Cheng & Thompson (2008) introduced more terms with special relevance to Microdontinae, which are used also in the present paper. For some other characters, terms derive from Hippa & Ståhls (2005) (e.g. antennal fossa, antetergite) and Speight (1987) (e.g. anterolateral callus of tergite 1, anterior sclerite of sternite 2). For the male genitalia, the terminology of McAlpine (1981) is supplemented following Sinclair (2000).

Morphological character matrix

The starting point for the morphological character matrix was Hippa & Ståhls (2005); many characters from this proved useful. Others were modified (e.g. extra character states were added), and some omitted because of irrelevance or for pragmatic reasons (see below). The numbering system of Hippa & Ståhls (2005) is indicated by the letters H&S, to avoid confusion with those in this matrix.

The following characters of Hippa & Ståhls (2005) were excluded from the present matrix because their state is the same for all (or all but one) of the studied taxa (state in parentheses): H&S # 010 (0, except 1 in *Syrphus*), H&S # 013 (0), H&S # 015 [1; some species of Microdontinae have a thickened arista, but this is of a quite different type than the species for which Hippa & Ståhls (2005) applied character state 1; therefore, this character statement is replaced in the current matrix by # 025], H&S # 036 (0, except 1 in *Merodon*), H&S # 019 (0, except 1 in *Eristalis*), H&S # 037 (0), H&S # 068 (0, except 2 in *Merodon*), H&S # 089 (0, except 1 in *Eristalis*), H&S # 118 (0), H&S # 119 (0).

Characters with the same state within all studied Microdontinae, but included because they vary in the outgroup (state in Microdontinae in parentheses) are: H&S # 010 (0), H&S # 014 (1), H&S # 019 (0), H&S # 021 (0), H&S # 038 (3), H&S # 053 (0), H&S # 065 (0), H&S # 066 (0), H&S # 067 (0), H&S # 081 (0), H&S # 089 (0), H&S # 096 (0), H&S # 099 (not applicable in Microdontinae, as male tergite 5 is always postabdominal), H&S # 100 (2), H&S # 104 (1), H&S # 105 (1), H&S # 106 (1), H&S # 110 (1), H&S # 112 (0), H&S # 113 (0), H&S # 114 (1), H&S # 117 (0).

Some character statements of Hippa & Ståhls (2005) were revised: character statements H&S # 041 and H&S # 042 were replaced by character 065, which describes more adequately the character states as they occur in Microdontinae. Character statement H&S # 069 was replaced by character 145.

Characters of Hippa & Ståhls (2005) requiring special specimen preparation were excluded including those requiring SEM imaging (H&S # 064, H&S # 073, H&S # 076, H&S # 077, H&S # 078, H&S # 079) and some from male or female postabdomens (H&S # 101, H&S # 102, H&S # 103, H&S # 107, H&S # 108, H&S # 109, H&S # 115, H&S # 116). Thus, the present matrix includes 78 characters of Hippa & Ståhls (2005) and 96 new characters, summing up to 174.

Notation of character statements

Following Sereno (2007), we distinguish between characters (as independent variables) and character states (as mutually exclusive conditions of a character). The description of a character is subdivided hierarchically into a secondary locator L2 (e.g. antenna), a primary locator L1 (e.g. basoflagellomere), a variable V (e.g. length) and a variable qualifier q (e.g. length relative to scape). The states are given subsequently following a colon. A secondary (or even tertiary) locator is added only to clarify the position of the primary locator. In the example given above, the entire character statement could be as follows: Antenna, basoflagellomere, length relative to scape: shorter (0); as long as (1); longer than (2).

Drawings and photographs

Male genitalia were dissected and macerated in an aqueous 10% KOH solution at ambient temperature for 12–24 h and stored in glycerol, in microvials attached to the original specimen. Drawings of male genitalia were made with the aid of a drawing tube attached to a Wild M20 compound microscope. Digital photographs of (parts of) specimens were taken through an Olympus SZX12™ motorized stereozoom microscope, using Analysis Extended Focal Imaging Software.

Choice of molecular markers

For the molecular dataset, five sequence partitions of three molecular markers were used: two each for the mitochondrial *COI* gene and the nuclear ribosomal RNA gene *18S*, and one for the nuclear ribosomal RNA gene *28S*. Primer information and combinations are given below and in Table S2.

Molecular markers derived from previous studies on Syrphidae – a combination of mitochondrial *COI* and nuclear *28S* sequences with morphological characters – yielded good results in the study on the intrafamilial relationships of Syrphidae of Ståhls *et al.* (2003). The *18S* gene fragment used by Mengual *et al.* (2008) proved informative for reconstructing deeper branches in the study of relationships within the subfamily Syrphinae.

DNA extraction

For most specimens, two or three legs were used for DNA extraction. In a few cases the entire thorax or the abdomen was used. Prior to extractions, ethanol-preserved samples were rinsed in distilled water.

DNA extractions were made using the NucleoSpin® Tissue extraction kit, following the manufacturer's protocol, eluting

the DNA into 50 µL of elution buffer. For some very small specimens NucleoSpin® Tissue XS was used, which involves the same extraction procedures, except for some differences in the quantities of buffers and washing liquids.

PCR

For all gene fragments, PCR amplifications were made using 4–8 μL of DNA-extract, suspended in a total volume of 25 μL reaction mix also containing 2.5 μL of 10X Buffer II, 2 μL mM $MgCl_2$, 4 μL 200 mM dNTP, 0.25 μL of Taq DNA polymerase, ultrapure H_2O (volume dependent on volume of DNA-extract) and 1 μL each of two primers (at 10 pmol/μL). The primers used for the amplified gene fragments are listed in Table S2. The following combinations were used: *COIa*: LCO + HCO or the smaller fragment Beet + HCO; *COIb*: Jerry-Pat or the smaller fragment Jerry + Inger; *18S*: the full fragment 1F + b3.9 or the two overlapping fragments 1F + b7.0 and 2F + b2.9; *28S*: F2 + 3DR. For many samples, attempts to amplify larger gene fragments (e.g. LCO + HCO and Jerry + Pat for *COI*, or 1F + b3.9 for *18S*) failed. For this reason, only the smaller fragments were amplified (e.g. Beet + HCO for *COI*, or 1F + b7.0 for *18S*).

For all amplifications, the following thermocycler profile was used: (step 1) 2 min at 95°C, (step 2) 1 min at 94°C, (step 3) 30 s at 49°C, (step 4) 2 min at 72°C, (step 5) repeat steps 2–4 for 30 times, (step 6) 7 min at 72°C, (step 7) cool down for some minutes at 4°C.

The PCR products were visualized by running 4-μL PCR products on a 1.5% agarose gel. PCR products were treated with ExoSapIt prior to sequencing reactions. Sequencing electrophoresis was carried out in the sequencing service laboratory of the Finnish Institute for Molecular Medicine (FIMM), University of Helsinki, Finland, with an ABI3730xl DNA Analyzer.

Sequences of forward and reverse primers were assembled and edited in Sequence Navigator v1.01 (Applied Biosystems, Foster City, CA). For the outgroup taxon *Chalarus spurius* (MZH-voucher Y0800), the *COIb* sequence was not available, for which reason the sequences of this taxon were combined with the *COIb* sequence of *Chalarus* sp. (MZH-voucher Y0038).

Alignment

The mitochondrial DNA sequences of the (protein coding) *COIa* and *COIb* gene fragments were aligned manually by their codon positions. Sequences of the *18S* and *28S* ribosomal RNA genes were aligned separately using MAFFT v6 (Katoh *et al.*, 2002, 2009; Katoh & Toh, 2008). This program offers several algorithms, some of which perform very well compared to those of other programs (e.g. ClustalW, DIALIGN-T, T-COFFEE) for multiple sequence alignment (Golubchik *et al.*, 2007; Rosenberg, 2009). We used E-INS-i: based on Katoh & Toh (2008) and Katoh *et al.* (2009), this algorithm was considered most suitable for ribosomal DNA sequences as it was developed for dealing with sequences with considerable length variation.

Datasets and analyses

Phylogenetic analyses were made by both parsimony and Bayesian analyses.

Parsimony analyses were performed using the software program TNT (Tree Analysis using New Technologies) v1.1, October 2010 (Goloboff *et al.*, 2008b), with gaps treated as missing data and morphological characters treated as nonadditive. Two sets of taxa were used (with the same set of morphological characters): a set containing all 189 taxa (the 'total set') and a set containing only the 90 taxa for which DNA data are available (the 'subset').

All molecular markers were analysed separately and sequences with remarkable placements (e.g. ingroup taxa in the outgroup) were scrutinized for possible errors in the sequences, such as copy–paste errors in the datafiles or contamination during DNA extraction or amplification. A few suspect or erroneous sequences were omitted subsequently from further analyses.

A single matrix integrating the data of all three molecular markers (in five fragments) then was constructed, which contained 90 taxa and 2740 columns of nucleotide data (including gaps). The TNT search for this matrix was stopped after the shortest length was found 50 times. Molecular and morphological datasets were merged using the *dmerge* command in TNT, resulting in a concatenated matrix of 2740 molecular sites and 174 morphological characters.

Combined matrices were analysed using a combination of all four 'new technology' heuristic search methods of TNT, under their default parameters: sectorial search, parsimony ratchet, tree-drifting and tree-fusing (see, e.g., Goloboff *et al.*, 2008b for explanations on commands). Searches were set to stop when minimum tree length was hit 100 times for the subset and 30 times for the total set.

Morphological characters of the total set of taxa were subjected to parsimony analyses under 'implied weighting' (Goloboff, 1993; Goloboff *et al.*, 2008a), a method which downweights characters according to their degree of homoplasy. The strength of the weighting function is determined by constant value k in the implied weighting formula. The approach used here derives from Mirande (2009), who explored a range of k-values. In this approach, the chosen k-values were not distributed regularly, because – as Mirande (2009) argues – this results in an artificial bias of the results towards the higher k-values. This bias is avoided by choosing k-values such that the values of fit (F) produced by the trees obtained under different k-values are divided into regular intervals. Here, as in Mirande (2009), k-values were chosen so as to result in average character fits of 50, 54, 58, 62, 66, 70, 74, 78, 82, 86 and 90%.

In order to obtain k-values, the formula for implied weighting was rewritten as $[k = (F \times S)/(1-F)]$. S is a measure of the average homoplasy per character, calculated as [S = (number of observed steps) – (minimum number of steps)/(number of characters)]. The number of observed steps is based on the shortest trees found under equal weights (2292 for the total set of 189 taxa). The minimum number of steps is the cumulative number of minimum character state changes for all 174 characters, which amounts to 242. So, the value of S used for the total set of taxa is (2292 to 242)/174 = 11.78. The resulting k-values are listed in Table S3. As in Mirande (2009), the most stable trees are considered to be those four which share the highest number of nodes with the other trees, as measured by the SPR-distance (Goloboff, 2008) and the distortion coefficient sensu Goloboff *et al.* (2008b) (DCG), which was determined using the *tcomp* command in TNT. A strict consensus tree was derived from these four trees.

For Bayesian analyses, MrBayes v3.2 was used (Huelsenbeck & Ronquist, 2001; Ronquist & Huelsenbeck, 2003). Molecular data were divided into nine partitions: *18S* 1, *18S* 2, *28S*, and three for each codon position of *CO1* a and *CO1* b. The general time reversible nucleotide substitution model with invariant gamma (GTR + I + G) was applied to these sequences, with separately calculated sets of parameters for each partition. The morphological dataset was analysed under the mk1 model (Lewis, 2001), with coding set to variable. Each analysis consisted of two independent simulations of four simultaneous MCMC chains, sampling every 1000th generation. Convergence was reached after 20 million generations with 0.038 (molecular data only) and 0.014 (molecular and morphological data combined) standard deviation of split frequencies, as suggested by Ronquist *et al.* (2011). The initial 5000 trees (25%) were discarded as burn-in. Majority-rule consensus trees were computed with posterior probabilities for each node.

Measures of support and stability

Bremer support values were calculated by TBR branch swapping based on the strict consensus trees, using the 'Bremer supports' option under the 'Trees' menu, examining trees up to 100 steps longer than the most parsimonious trees. Jackknife values and GC frequency differences (Goloboff *et al.*, 2003) were calculated in TNT, using 1000 replicates and a removal probability of 36%. GC values indicate the difference between the frequency in which nodes are retrieved in the jackknife replicates and the frequency of the most frequent contradictory group. So, in contrast to normal jackknife values, the GC values are informative for the amount of contradictory information in the dataset. If these values are equal, there are no contradictory groups that are supported by the data. For Bayesian inference, posterior probability values are indicated.

Results

Character statements and matrix

A list of all character statements is given below and character state matrix provided in Table S4.

Head

000. Face, shape, lateral view: simple (0) (Fig. 1); concave (1); sexually dimorphic: tuberculate in male, concave in female (2); tuberculate (3) (Fig. 2). H&S # 000.
Most species of Microdontinae have a simple, untuberculate face and sexual dimorphism does not occur in this character. A tuberculate face occurs only in *Spheginobaccha* and *Eurypterosyrphus*. States 1 and 2 were not found among Microdontinae.

001. Face, pilosity: entirely pilose (0); pilose with a bare medial stripe (1); only laterally pilose (2); bare (3). H&S # 002.
A very narrow bare stripe (up to half the width of the antennal fossa) is coded as 0.

002. Face, medially, texture: smooth (0); transversely wrinkled (1) (Fig. 3).
If face has a bare medial stripe, even only very narrow, the texture of this bare part can be transversely wrinkled.

003. Face, pollinosity: not pollinose (0); laterally narrowly pollinose (1) (Figs 4, 5); widely pollinose (2).

004. Eyes, contiguity in male: holoptic (0); dichoptic (1). H&S # 006.
All known Microdontinae have dichoptic males, although distance between the eyes may be very small (e.g. *Hypselosyrphus amazonicus*, Fig. 4). Holoptic is used for specimens in which the eyes are partly contiguous on top of the head.

005. Face, frontal view, width relative to eye: narrower than an eye (0) (Figs 4, 5); as wide as an eye (1) (Fig. 6); wider than an eye (2) (Figs 7, 8).
This character is not always easy to assess. Doubtful cases are coded as 1. As the width of the face is often sex-dependent, this character was scored for the male sex when available. If no male was available, the character either was not scored or estimated on a combination of female face width or extrapolated from closely related species.

006. Eyes, margins, degree of convergence in male: converging at transition between frons and vertex (0) (Figs 4, 6, 8); straight, without sign of convergence (1) (Fig. 9).

007. Antenna, length relative to face: shorter than (0) (Figs 10, 13); as long as (1) (Fig. 11); longer than (2) (Figs 12, 25) distance between antennal fossa and anterior oral margin.

008. Antenna, basoflagellomere in male, furcation: not furcate (0) (Figs 10–12); bifurcate (1) (Figs 7, 14); multifurcate (2) (Fig. 15).
Within Syrphidae other than Microdontinae, a furcate basoflagellomere is known only in *Cacoceria* Hull. Within the Microdontinae found in several Neotropical,

Figs. 1-8. Head male, lateral view. (1) *Peradon bidens*; (2) *Eurypterosyrphus* sp; (3) *Microdon bidens*, male. Face medially with transversely wrinkled texture; (4) Head, frontal view. *Hypselosyrphus amazonicus* male; (5) *Hypselosyrphus* sp. female; (6) *Peradon bidens* male; (7) *Carreramyia megacephalus* male; (8) *Metadon mynthes* male (A, arista).

few Oriental and Australian taxa. In most known species concerned, this occurs only in the male, except in *Masarygus carrerai* Papavero and *Johnsoniodon malleri* Curran.

009. Antenna, scape, length relative to width: short, maximally 2× as long as wide (0) (Fig. 13); elongated, > 2× as long as wide (1) (Figs 10–12). H&S # 012.
010. Antenna, pedicel, length relative to width: maximally 1.5× as long as wide (0) (Figs 10–10–12, 16); at least 2× as long as wide (1) (Fig. 17).
011. Antenna, basoflagellomere, length relative to width: short, maximally 2× as long as wide (0) (Figs 10, 13); elongated, > 2× as long as wide (1) (Figs 4, 11, 12, 14, 15).
012. Antenna, basoflagellomere, length relative to scape: shorter than (0) (Figs 2, 10, 17); as long as (1); longer than (2) (Figs 12–16) scape.
013. Antenna, basoflagellomere, shape: not sickle-shaped or laterally flattened (0) (Figs 10–17); sickle-shaped (1) (clearly narrower at apex than at base, with dorsal margin straight or concave and ventral margin convex; Fig. 18); strongly swollen, but not sickle-shaped (2) (Fig. 2); laterally flattened and greatly widened (more than 1.5 times as wide as apical part of scape) (3) (Fig. 19).
014. Antenna, basoflagellomere, presence of pilosity with length at least half the diameter of the basoflagellomere: absent (0) (Figs 10–19); present (1) (Fig. 20).
015. Antenna, arista, insertion: dorsal (0), lateral (1). H&S # 014.
016. Antenna, arista, length: absent (0) (Figs 7–15, 14); maximally as long as pedicel (1) (Fig. 14); longer than pedicel (2) (Figs 16–19).
017. Antenna, arista, shape: normal (0) (Figs 13, 16, 18, 19); thickened, medially clearly wider than basal width (1) (Fig. 8).

Figs. 9-18. *Rhoga sepulchrasilva*, head male. (9) frontal view; (10) lateral view; (11) Head male, lateral view; *Stipomorpha tenuicauda*; (12) *Rhopalosyrphus guentherii*; (13) *Paramicrodon lorentzi*; (14) Antenna, male. *Schizoceratomyia barretoi* (A, arista); (15) *Masarygus palmipalpus*; (16) *Peradon bidens*; (17) *Microdon rufiventris*; (18) *Menidon falcatus*.

018. Antenna, arista, pilosity, length: absent or short (0); at least half as long as diameter of arista (1); long only dorsally and ventrally (2). H&S # 018.
019. Antennal fossa, width: as wide as high or higher than wide (0); clearly wider than high (1). H&S # 011.
Whereas in most Syrphidae the antennal fossa is clearly wider than high (Hippa & Ståhls, 2005), in most Microdontinae the antennal fossa is as wide as high or (sometimes) higher than wide.
020. Face, shape, lateral view: straight or evenly convex, sometimes with facial tubercle (0) (Figs 1, 2, 10, 11, 20); ventrally bulging and prominent (1) (Fig. 12).
021. Mouth parts, degree of development: undeveloped, oral opening not or hardly visible (0) (Fig. 21); mouth parts developed (1) (Figs 22, 23).
Mouthparts of Microdontinae vary in development, but only in a few are they reduced such that there is no oral opening.
022. Oral margin, laterally, degree of development: produced, anteriomedially notched (0) (Figs 1, 6, 11, 12, 24); not produced (1) (Figs 4, 5, 8, 9, 10, 13, 22, 23). H&S # 001.
023. Gena, degree of development: developed (0) (Fig. 22); not or hardly developed, eyes bordering (almost) directly on oral margin (1) (Fig. 23).
024. Vertex, shape: not produced (0) (Figs 1, 2, 6, 8, 12, 13, 19); convex and shining (1) (Figs 4, 5, 9, 10, 11, 24); produced but not convex and shining (2) (Figs 20, 25).
025. Vertex, pilosity: bare (0); pilose (1).
026. Vertex, frontal ocellus, shape: round (0); oval ($\geq 1.5\times$ as wide as long) (1); divided in two (2) (Fig. 28); absent (3).
027. Occiput, dorsal half, width: not widened (0) (Figs 26, 27); widened (1) (Figs 1, 10, 11, 12, 13, 20, 24, 25).
Coding of this character was strict: only if the dorsal half of the occiput was not widened over its entire length was

state 0 scored; state 1 for slightly widened dorsal half of the occiput (Figs 1, 11), and taxa in which the dorsal half of the occiput was strongly swollen (Figs 10, 20).

028. Occiput, ventral half, width: not widened, much narrower than length of ocellar triangle (0) (Figs 1, 11, 12, 13, 20); widened, about as wide as length of ocellar triangle or wider (1) (Figs 10, 27).
029. Eye, posterior margin, shape: convex or straight (0); concave (1). H&S # 008.
030. Eye, pilosity, length: long (0); intermediate (1); short or absent (2). H&S # 007.

Thorax

031. Thorax, pile, shape: unbranched (0), branched (1). H&S # 021.
032. Postpronotum, pilosity: bare (0); pilose (1). H&S # 032.
033. Prothorax, prothoracic basisternum, dorsal part, shape: sub-quadrangular (0); trapezoidal (1); sub-triangular (2). H&S # 025.
034. Prothorax, prothoracic basisternum, ventrolateral corners, shape: rounded (0) (Fig. 29); bluntly angular (1) (Fig. 30); sharply angular or with sharp spine (best visible in lateral view) (2) (Fig. 31).
035. Prothorax, prothoracic basisternum, pilosity: bare (0); pilose (1). H&S # 026.
Microtrichia are not coded as pilosity.
036. Prothorax, antepronotum, anterodorsal margin, degree of development: underdeveloped (0); with collar-like thickening (1). H&S # 027.
Hippa & Ståhls (2005) consider a median incision as an implicit part of character state 1, but in Microdontinae this is not always true, so here these are coded as separate characters.
037. Prothorax, antepronotum, anterodorsal margin, presence of median incision: absent (0); present (1).
See notes at # 036.
038. Prothorax, antepronotum, anterodorsal margin, pilosity: bare (0); pilose (1).
039. Prothorax, propleuron, shape: flat (0); produced laterally (1). H&S # 028.
040. Prothorax, propleuron, ventral part, pilosity: bare (0); pilose (1). H&S # 029.
041. Prothorax, propleuron, dorsal part, pilosity, uniformity of length: uniform (0); with longer fine and intermixed shorter spine-like pile (1); almost nonpilose (2). H&S # 030.
042. Prothorax, propleuron, dorsal part, pilosity, arrangement: scattered (0); in a vertical row (1). H&S # 031.
043. Prothorax, posterior cervical sclerite, position: ventral (0); dorsal (1). H&S # 022.
In some cases the posterior cervical sclerite is not or hardly visible, because the prothoracic basisternum is very close to the lateral cervical sclerite. These cases are coded as 1.
044. Prothorax, posterior cervical sclerite, shape of apex: concavely cut (0); acute or rounded (1). H&S # 023.
045. Prothorax, cervical membrane, pilosity: bare (0); pilose (1). H&S # 024.
046. Propleuron, pilosity: bare (0); pilose (1).
047. Anepisternum, median part, sulcus, degree of development: no sulcus (0) (Figs 32, 33); sulcate (1) (Fig. 34).
State 0 was coded only for taxa in which the entire anepisternum is convex or near-flat. There is a continuous variation between taxa with only a slightly sulcate anepisternum and a deeply sulcate anepisternum. Even if there is only a slight sulcus close to the posterior margin of the anepisternum is slightly raised, the state of this character is coded as 1.
048. Anepisternum, anterior part, pilosity: bare (0) (Fig. 35); pilose (1) (Figs 32, 33, 34).
049. Anepisternum, posterior part, pilosity: bare (0) (Figs 33, 35); pilose (1) (Figs 32, 34).
050. Anepisternum, pilosity: entirely pilose or with bare part limited to ventral half (0) (Fig. 32); widely bare ventrally, with bare part reaching dorsad to at least half the height (1) (Figs 33, 34).
051. Thorax, texture of pilosity: soft pile (0); bristly pile or intermixed soft and bristly (1). H&S # 020.
052. Anepimeron, anterior part, pilosity: bare (0) (Fig. 35); pilose (1) (Figs 32–34).
053. Anepimeron, anterior part, pilosity, distribution: limited to dorsal half (0) (Fig. 33); also pilose on ventral half (1) (Figs 32, 34).
054. Anepimeron, dorsomedial part, microtrichosity: absent (0); present (1).
055. Anepimeron, posterior part, microtrichosity: absent (0); present (1).
056. Katepisternum, dorsal part, pilosity: bare (0); pilose (1).
In Hippa & Ståhls (2005) (# 44), pilosity of the katepisternum is coded into one character statement. In Microdontinae, the katepisternum is never entirely pilose: the dorsal and ventral patches of pile are always widely separated. The dorsal pilosity always is close to the dorsal margin, whereas ventral pilosity is mostly very sparse and only found close to the ventral margin. Presence of pile on the dorsal part is here considered to be independent of presence of pile on the ventral part, and therefore are coded in separate statements (056 and 057).
057. Katepisternum, ventral part, pilosity: bare (0); pilose (1).
Only microtrichose is coded as 0. See notes under # 056.
058. Katepimeron, pilosity: pilose (0); bare (1). H&S # 046.
059. Katepimeron, texture: smooth (0); wrinkled (1).
Partly wrinkled is coded as wrinkled.
060. Katepimeron, shape: flat (0); convex (1). H&S # 045.
061. Metaepisternum, pilosity: bare (0); pilose (1). H&S # 055.
Within the Microdontinae, a pilose metaepisternum has only been found in *Microdon contractus* Brunetti and *M. conveniens* Brunetti.
062. Katatergum, microtrichosity, length: absent (0); short microtrichose (1); long microtrichose, much longer than

Figs. 19-27. Head male, lateral view. (19) Undescribed genus #1 species AUS-01; (20) *Ceratrichomyia behara*; (21) Head male, ventral view. *Masarygus palmipalpus*; (22) *Schizoceratomyia barretoi*; (23) *Rhoga sepulchrasilva*; (24) Head male, lateral view. *Pseudomicrodon batesi*; (25) *Carreramyia megacephalus*; (26) *Hypselosyrphus* sp.; (27) *Hypselosyrphus ulopodus*.

on anatergum (2). H&S # 049 (one character state added and coding adapted).

The only known Syrphidae without microtrichia on the katatergum are found in the Microdontinae: *Surimyia* Reemer and a new species of *Masarygus*.

063. Katatergum, microtrichosity, arrangement: uniform (0); arranged as oblique dorsoventral stripes (1). H&S # 050.
064. Anatergum, microtrichosity: absent (0); present (1).
065. Katatergum, posterior margin, presence of carina: absent (0); present (1). H&S # 048.

A carina on the posterior margin of the katatergum was found only in *Microdon granulatus* Curran and *Chrysidimyia chrysidimima* Hull.

066. Mediotergite, subscutellum, degree of development: absent (0); rudimentary (1); fully developed (2). H&S # 039 ('arciform crest' of metanotum).
067. Mediotergite, microtrichosity, extent: entirely (0); intermediate (1); bare (2). H&S # 040.
068. Metasternum, degree of development: underdeveloped (0); intermediate (1); well-developed (2). H&S # 056.
069. Metasternum, pilosity: bare (0); pilose (1) H&S # 057.
070. Metapleura, contiguity: separated (0); touching in one point (1); forming a complete postmetacoxal bridge (2). H&S # 058 (one character state added).

Absence of a 'postmetacoxal bridge' was known only from *Spheginobaccha* (Cheng & Thompson 2008) but we show that certain species of *Rhoga* also have the metapleura separated. In two other taxa (*Ceratophya variegata* Hull and *Surimyia*) the metapleura seem to be touching only at one point, complicating the character state assessment. For these cases, character state 1 was added.

071. Metepimeron, abdominal spiracle, position: embedded (0); not embedded (1). H&S # 061.
072. Metepimeron, abdominal spiracle, presence of fringe of long microtrichia: absent (0); present (1) (Fig. 36).

In most Microdontinae, the abdominal spiracle in the metepimeron is surrounded by a dense fringe of long microtrichia, often forming a sort of tuft. In a few taxa this fringe is absent.

073. Mesonotum, transverse suture, presence: absent or only weakly visible at notopleuron (0); well-developed, but incomplete and may be short (1); complete (2).
074. Mesonotum, anterolaterally at transverse suture, tubercle: absent (0); present (1). H&S # 033.
An anterolateral tubercle on the mesonotum was not found in Microdontinae.
075. Mesonotum, notal wing lamina, degree of development: underdeveloped (0); developed (1); strongly developed (2). H&S # 034.
076. Integument ventral of postalar callus, tubercle: absent (0); present (1). H&S # 035.
A tubercle on the integument ventral of the postalar callus was not found in Microdontinae.
077. Plumule, degree of development: long (> 4× longer than wide) (0); short (1); absent (2). H&S # 052.
As the plumule is an extension of the posterior part of the subalar sclerite, varying strongly in degree of development among the taxa, character states 1 and 2 are sometimes difficult to assess. In some taxa of Microdontinae, short microtrichia are present on a hardly developed posterior part of the sclerite. In these cases it can be difficult to decide whether to regard this structure as a short plumule or merely as a microtrichose posterior part of the subalar sclerite, in which case the plumule is considered to be absent. Character state 0 does not occur among Microdontinae.
078. Plumule, microtrichia, length: short (0); longer than diameter of anterior part of subalar sclerite (1); absent (2).
079. Plumule, vestiture, shape: simple (0), simple with bifurcate (1), multifurcate (2). H&S # 053.
080. Subalar sclerite, anterior part, width relative to posterior part: about as wide (0) (Fig. 37); wider (1) (Fig. 38); narrower (2).
081. Subalar sclerite, anterior part, length relative to posterior part: longer (0) (Fig. 37a); as long as (1) (Fig. 37b); shorter (2) (Fig. 37c).
082. Subalar sclerite, anterodorsal process, shape: simple (0); apically dilated (1); apically strongly dilated (2). H&S # 051.
Character state 2 was not found among Microdontinae.
083. Posterior spiracle, exposure in lateral view: exposed (0); directed posteriorly, not wholly exposed (1). H&S # 047.
084. Scutellum, apical calcars: absent (0); present (1) (Figs 39–41).
Many species of Microdontinae have two apical extensions of the scutellum. Following Thompson (1999), these extensions are here called calcars.
085. Scutellum, apical calcars, shape: normal, spine-like (0) (Fig. 39); dorsoventrally flattened and blunt (1) (Fig. 40); extremely large and conical (2) (Fig. 41).

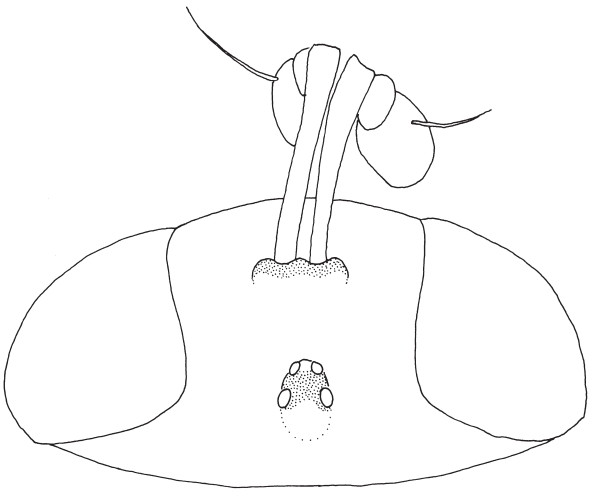

Fig. 28. *Stipomorpha wheeleri* male, head dorsal.

There is a large variation in shape, size and mutual distance of the scutellar calcars of Microdontinae. Most of this variation cannot be coded into discrete states, except for those described here. In taxa in which scutellar calcars are absent, coded as inapplicable.

086. Scutellum, shape: normal, more or less semicircular (0); apicomedially sulcate (1); triangular (2).
Important note: state 1 was coded only for taxa without calcars on the scutellum.
087. Scutellum, angle with mesonotum: at same level (0); making angle of at least 30° (1).
088. Scutellum, subscutellar hair fringe: several rows of hairs (0), one to two rows of hairs (1), incomplete (2), absent (3). H&S # 038.

Wings

089. Calypter, size: wider than basal length (0); intermediate (1); narrow strip (2). H&S # 092.
090. Calypter, ventral lobe ventrally, pilosity: bare (0); pilose (1). H&S # 094 (character states coded inversely).
091. Alula, degree of development: normal, large (0); narrow strip (1); rudimentary or absent (2) H&S # 074.
092. Alula, microtrichosity: entirely bare (0); partly bare (1); entirely microtrichose (2).
093. Vena spuria, presence: absent or nearly so (0); weak (1); strong (2). H&S # 075.
094. Vein Sc, apex, position: proximal of (0) (Figs 42, 45, 46); at same level as (1) (Figs 43, 49); distal of rm (2) (Figs 44, 48, 50).
Doubtful cases are coded as 1.
095. Vein R1, apex before joining costal vein, shape: straight or only slightly curved (0) (Figs 42–44, 46, 49, 50); curved anteriad (1) (Figs 45, 48).
096. Vein RS, occupation with setae: on entire length (0); only on basal part (1); only on apical half (2). H&S # 086.

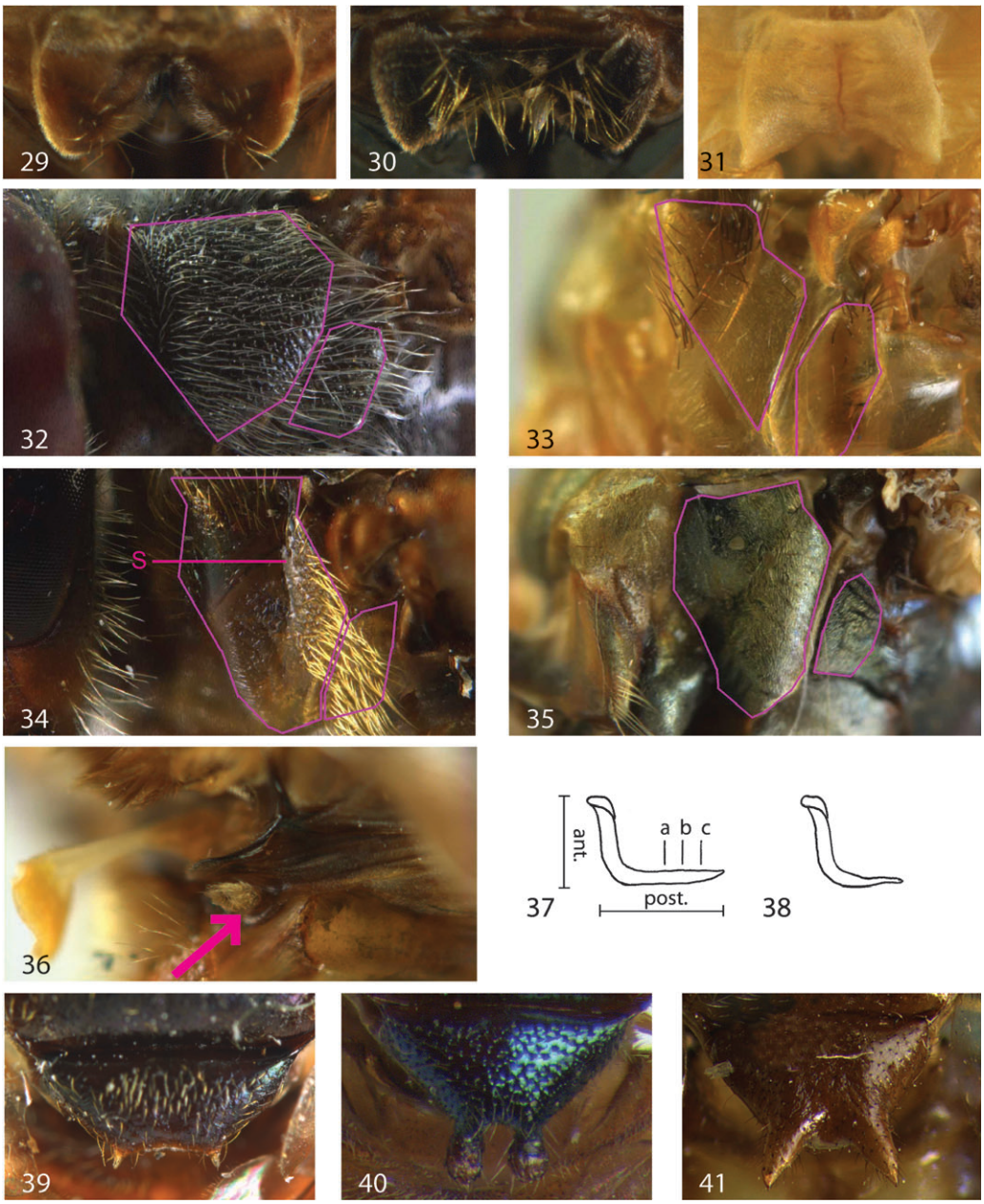

Figs. 29-41. Prothoracic basisternum, frontal view. (29) *Peradon bidens*; (30) *Microdon rufiventris*; (31) *Carreramyia megacephalus*; (32) Anepisternum and anepimeron. *Rhopalosyrphus guentherii*; (33) *Stipomorpha mixta*; (34) *Peradon luridescens* (S, sulcus); (35) *Spheginobaccha macropoda*; (36) *Peradon bidens*, metepimeron, ventral view, with first abdominal spiracle embedded and with fringe of long microtrichia. (37) Subalar sclerite. Anterior part about as wide as posterior part, longer than (a), as long as (b), shorter than (c), posterior part; (38) Anterior part wider than posterior part; (39) Scutellum, dorsal view. *Peradon bidens*; (40) *Hovamicrodon nubecula*; (41) *Megodon stuckenbergi*.

Among Microdontinae, no taxa were found with setae on vein RS.

097. Vein R2 + 3, base, shape: straight (0); bowed in proximal part (1) (Fig. 51). H&S # 080.
In all examined Microdontinae, vein R2 + 3 is bowed in the proximal part. This is explained in Fig. 51.

098. Vein R2 + 3, apex, position: proximal of (0) (Figs 43, 48, 50); at same level as (1) (Figs 46, 49); distal of (2) (Figs 42, 44, 45) junction of M1 and R4 + 5.
Doubtful cases are coded as 1.

099. Vein bm-cu, length relative to basal section of CuA1: shorter (0) (Figs 43, 44, 46, 48); about equally long (1) (Fig. 49); longer (2) (Fig. 47). H&S # 088.

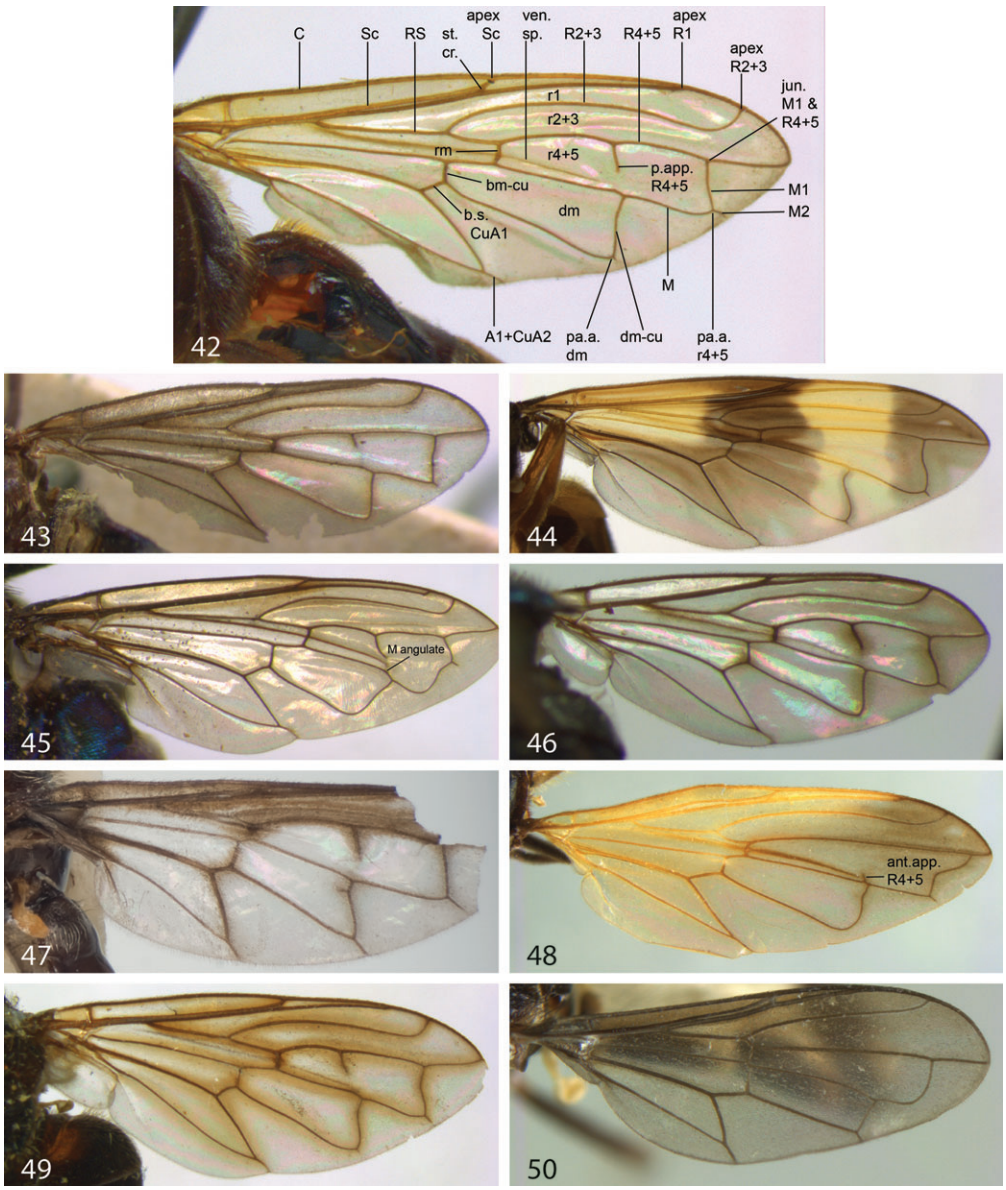

Figs. 42-50. Wing. (42) *Stipomorpha inarmata*; (43) *Archimicrodon venosus* Walker; (44) *Hypselosyrphus* sp.; (45) *Microdon* (*Chymophila*) *instabilis*; (46) *Hovamicrodon silvester*; (47) Undescribed genus #1 species AUS-01; (48) *Aristosyrphus primus*; (49) *Archimicrodon nigrocyaneus*; (50) *Masarygus palmipalpus*. Codes: A, anal vein; ant.app., anterior appendix; b.s., basal section; C, costal vein; Cu, cubital vein; dm, discal medial cell; jun., junction; M, medial vein; pa. a., postero-apical angle; p.app., posterior appendix; R, radial vein; Sc, subcostal vein; st. cr., stigmal crossvein; ven. sp., vena spuria.

100. Marginal crossveins M1 and dm-cu: strongly disjunct (0); intermediate (1); contiguous or nearly contiguous (2). H&S # 083.
101. Vein M2, presence beyond junction with M1: present and extending to wing margin (0); present but not reaching wing margin (1) (Figs 42, 48, 49); not present (2) (Figs 45, 50).
102. Vein CuA1, presence beyond junction with dm-cu: present and extending to wing margin (0) (Figs 47, 50); present but not reaching wing margin (1) (Figs 44, 49); not present (2) (Figs 43, 45, 46, 48). H&S # 084.
103. Cell r4 + 5, apex: open (0); closed (1). H&S # 090.
104. Cell r4 + 5, posterior apical angle, shape: angular (0) (Figs 42–44, 46–49); roundly angular, but distinct (1); widely rounded or absent (2) (Figs 45, 50).
105. Cell dm, posterior apical angle, shape: angular (0) (Figs 42, 44, 47, 49, 50); roundly angular, but distinct (1) (Figs 43, 46); widely rounded or absent (2) (Figs 45, 48). H&S # 091

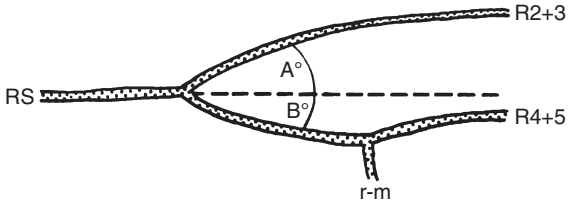

Fig. 51. Wing veins in Microdontinae (wing base on left side). The dashed line indicates an (imaginary) apical extrapolation of vein RS. In Microdontinae, vein R2 + 3 is strongly curved basally, resulting in angle A always being larger than angle B.

106. Vein M1, shape: straight, evenly curved or with slight inward angle (0) (Figs 42–44, 46, 47, 49, 50); strongly recurrent in anterior one third, often with small appendix (1) (Fig. 45); directed outward in anterior one third to one half (2) (Fig. 48).
107. Vein R4 + 5, shape: straight or shallowly looped (0), deeply looped (1). H&S # 081.
108. Vein R4 + 5, posterior appendix into cell r4 + 5, presence: absent (0) (Figs 44, 48, 50); present (1) (Figs 42, 43, 45–47, 49). H&S # 082.
109. Vein R4 + 5, posterior appendix into cell r4 + 5, position: proximal (0) (Fig. 49); intermediate (1) (Figs 43, 45–47); distal (2) (Fig. 42) of middle of cell R4 + 5.
110. Vein R4 + 5, apex, position: anterior of (0) (Figs 43, 45, 46, 48, 49); at (1) (Figs 42, 44, 50) wing apex.
111. Vein M, anterior appendix into cell r4 + 5, presence: absent (0) (Figs 42–47, 49, 50); present (1) (Fig. 48).
Character state 1 is found only in *Mixogaster*, *Sphegina-nobaccha* and some specimens of *Aristosyrphus primus* (Fig. 48).
112. Vein M, part between rm and dm-cu, shape: straight or evenly curved (0) (Figs 42–50–42–50, 42–44, 46, 47, 49, 50); angulate towards apex of vena spuria (1) (indicated in Fig. 45, see also 48).
113. Stigmal crossvein, presence: absent (0); present (1)
114. Cross-vein rm, position relative to cell dm: at basal one fifth or more apical (0) (Figs 42–46, 49); at basal one sixth or more proximal (1) (Figs 47, 48, 50).
115. Vein A1 + CuA2, shape: straight (0) (Figs 42, 47, 48, 50); curved (1) (Figs 44–46, 49); angulate (2); elongate and basally parallel to wing margin (3). H&S # 085 (character states modified).
Character states 2 and 3 were not found among Microdontinae.

Legs

116. Tibiae, basal cicatrices, presence: absent (0); present (1) (Fig. 52).
The term cicatrix (plural: cicatrices) was introduced by Hull (1949) to indicate the 'scar' that runs around the subbasal part of the femora and the subapical part of the tibiae of almost all Microdontinae. In some Syrphinae and Eristalinae, vague cicatrices can be seen on the femora, but never on the tibiae. In most, but not all, Microdontae the cicatrices on the tibiae are clearly visible.
117. Front- and mid-femora, proximal of cicatrix, density of pile/setae: as dense as on other anterior parts of femur (0); denser than on other anterior parts of femur (1).
The vestiture on the anterior side of the basal part of the front- and mid-femora, proximal of the cicatrix, is often more dense than the vestiture of the other anterior parts of the femur.
118. Front- and mid-femora, proximal of cicatrice, thickness of pile/setae: normal (0); spinose (1). H&S # 063.
As there is no straightforward division between the two states, the coding of this character is quite subjective. Although in many taxa the pile/setae under consideration are thicker than on other parts of the femur, state 1 was chosen only for few taxa.
119. Femora, ventral surface, pilosity: entirely pilose (0); with bare median stripe limited to apical half (1); with bare median stripe extended to basal half (2). H&S # 062.
Hippa & Ståhls (2005) recognized two states: either entirely pilose or with a median stripe over the entire length of the femur. In many Microdontinae, however, an intermediate state was found, in which the bare stripe is limited to the apical half of the femur. An extra state was added to account for this.
120. Hind femur, ventrally, presence of double row of spines: absent (0); present (1).
This character is similar to # 069 of Hippa & Ståhls (2005), but is described here because ventral spines on the hind femur are rare among Microdontinae.
121. Hind femur, anterobasal (called prolateral in Hippa & Ståhls 2005) sub-basal setae: undifferentiated (0), differentiated (1), spinose (2). H&S # 065.
122. Front tibia, apex, setae: long and irregular setae (0), placed in transverse comb-like row (1). H&S # 066.
123. Hind tibia, basoventral surface, shape: medially rounded or flat (0); keeled (1); double keeled or concave (2). H&S # 070 (descriptions of states 0 and 2 modified).
Among Microdontinae, a (double) keeled or concave hind tibia was not observed.
124. Hind tibia, basoventral surface, presence of setae: absent (0); with short, spinose setae (1). H&S # 071.
State 1 was found only in *Microdon nigrispinosus* Shannon.
125. Hind tibia, presence of long, dense pilosity dorsally and laterally: absent (0) (Fig. 52); present (1) (Fig. 53).
In several (mainly Neotropical) taxa the hind tibia is occupied with long, dense pile, reminescent of the corbicula of bees. In these taxa the hind tibia is often also strongly widened, which adds to the resemblance to bees.
126. Mid tarsus, basitarsomere, ventral vestiture: without spine-like setae (0), with pale spine-like setae (1), with dark spine-like setae (2). H&S # 067.
127. Hind basitarsus of male, dorsal view, width: as wide as (0); wider than (1) apex of hind tibia.

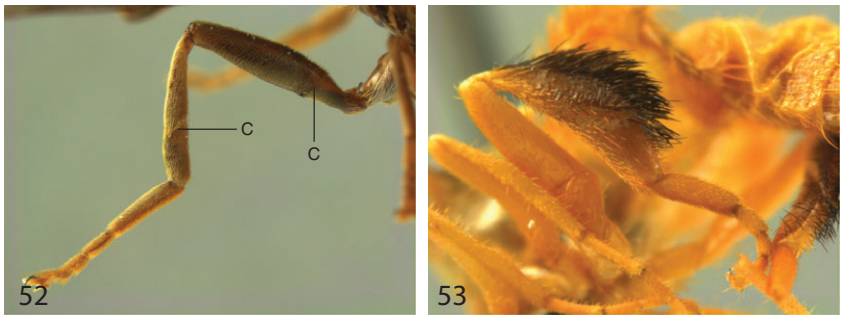

Figs. 52-53. Leg. (52) *Peradon luridescens*; (53) *Carreramyia megacephalus*.

This character is often sexually dimorphic: often state 1 is most pronounced in the male and less so or even absent in the female.

Abdomen

128. Abdomen, shape in dorsal view: not constricted (0); constricted with narrowest width before posterior margin of tergite 2 (1) (Fig. 54); constricted with narrowest width at posterior margin of tergite 2 (2) (Figs 55, 56).
129. Abdomen, tergites, lateral margins: unbordered (0), bordered (1). H&S # 096.
130. Tergite 2, ratio length/width: longer than wide (0) (Figs 54, 56); as long as wide (1) (Fig. 55); wider than long (2) (Figs 57, 58).
131. Tergite 3, ratio length/width: longer than wide (0) (Fig. 56); as long as wide (1); wider than long (2) (Figs 57, 58).
132. Tergite 4, ratio length/width: longer than wide (0) (Fig. 57); as long as wide (1); wider than long (2) (Fig. 58).
133. Antetergite, degree of fusing with tergite 1: free (0); almost free (1); almost fused with tergite 1 (2); indistinguishable or wholly fused with tergite 1 (3). H&S # 059.
134. Antetergite, presence of pilosity: bare (0); pilose (1). H&S # 060.
    If the antetergite is only microtrichose, this is coded as bare.
135. Tergite 1, anterolateral callus, presence: absent (0) (Fig. 59); present (1) (Fig. 60).
    The anterolateral corners of tergite 1 are often developed into a kind of turbercle or ridge, as if the tergite has been 'compressed' longitudinally. This structure, named the *callus of tergite 1* by Speight (1987), is best seen in dorsal view.
136. Tergite 2, lateral tubercle, presence: absent (0); present (1) (Fig. 61).
    The presence of a lateral tubercle halfway tergite 2 was observed only in *Ubristes* Walker.
137. Tergites 3 and 4, degree of fusing: not fused (0); fused (1). H&S # 097.
    In many cases, a clear suture is visible (especially medially) but the tergites do not articulate independently. These cases were coded as 1.
138. Tergite 5 in male, degree of incorporation in postabdominal segments: preabdominal (0); postabdominal (1). H&S # 098.
    In all Microdontinae under study, tergite 5 of the male is incorporated into the postabdominal segments. This character is shared with most Eristalinae, but distinguishes the Microdontinae from the Syrphinae (excluding the Pipizini).
139. Abdomen, male tergite 5, size and shape: large, normal (0), small, normal (1), sickle-shaped (2). H&S # 099.
140. Abdomen, male tergite 5, dextrolateral part: entire (0), dextro-apicolaterally obliquely folded (1), dextrosublaterally transversely folded (2). H&S # 100.
141. Abdomen, male segment 6, position: preabdominal (0), postabdominal (1). H&S # 104.
142. Sternites 2–4, width: normal, wide (0); much narrower than the tergites (especially 3 and 4), with wide lateral membraneous parts (1) (Fig. 62).
    State 1 was coded only for *Paramicrodon* Meijere, 1913. In taxa with a constricted abdomen (e.g. *Paramixogaster*, *Spheginobaccha*) the sternites also are narrow, but not much narrower than the tergites.
143. Sternite 1, pilosity: bare (0); pilose (1).
    The presence of pilosity on sternite 1 seems to be of good diagnostic value for certain genera or species groups, as little variation was found in this character among closely related species.
144. Sternite 2, anterior sclerite, presence: absent (0); present (1) (Figs 63, 64).
    In most Microdontinae and also in other syrphids, a narrow sclerotized strip is present in between sternites 1 and 2. Laterally, this strip is connected to sternite 2, thus apparently being part of it. The term *anterior sclerite of abdominal sternite 2* by Speight (1987) is also used here. When this sclerite can be considered as a part of sternite 2, indeed, then the sclerite could be named *acrosternite* of sternite 2, as explained in McAlpine (1981).
145. Sternite 2, anterior margin, shape: without median triangular incision (0) (Fig. 63); with median triangular incision (1) (Fig. 64).
146. Sternites 2 and 3, integument in between, width: normal (0) (Figs 63, 64); very wide (1) (Fig. 65).

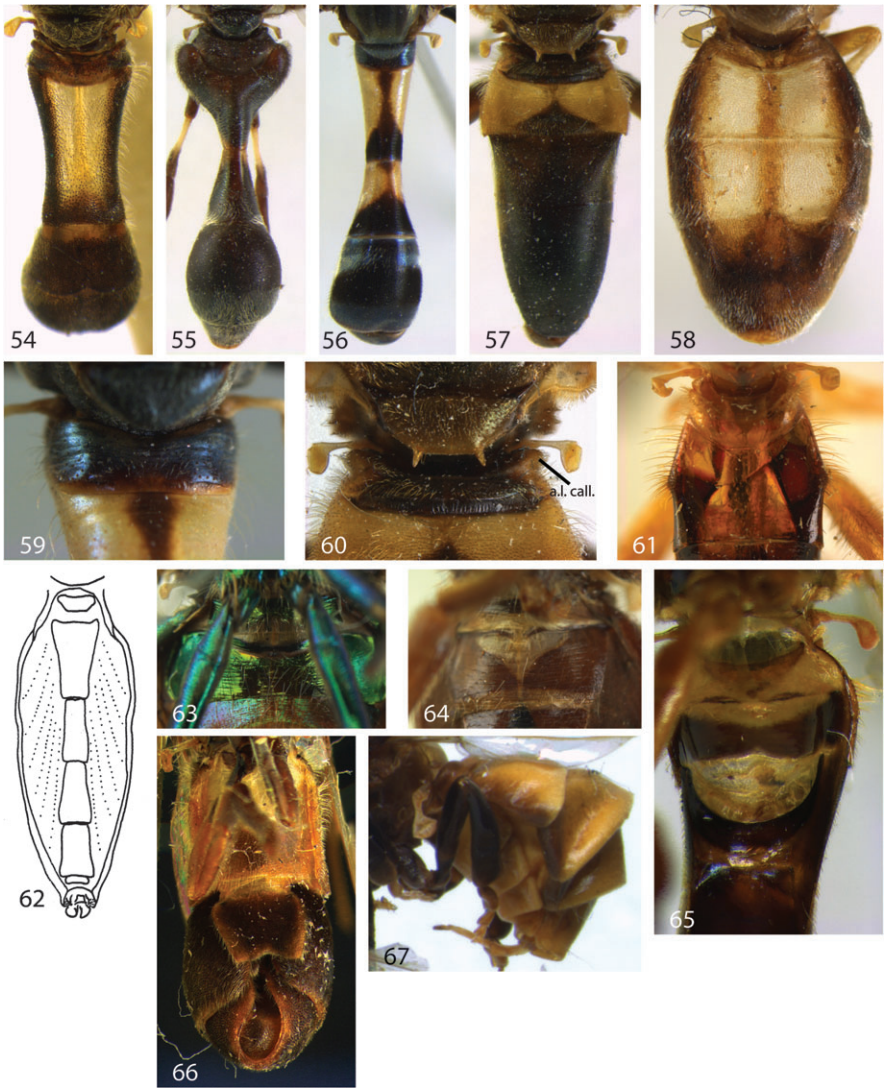

Figs. 54-67. Abdomen, dorsal view. (54) *Rhopalosyrphus cerioides*; (55) *Rhopalosyrphus guentherii*; (56) *Spheginobaccha macropoda*; (57) *Peradon luridescens*; (58) *Schizoceratomyia barretoi*; (59) Tergite 1, dorsal view. *Spheginobaccha macropoda*; (60) *Peradon luridescens*; (61) *Ubristes ictericus*, tergite 2, dorsal view; (62) *Paramicrodon* female, abdomen, ventral view; (63) Sternite 2, ventral view. *Microdon* (*Chymophila*) *instabilis*; (64) *Serichlamys mitis*; (65) *Stipomorpha goettei*; (66) *Kryptopyga pendulosa* male, abdomen, ventral view; (67) *Ceratophya panamensis* female, abdomen, lateral view.

In certain taxa, the integument between sternites 2 and 3 is much wider than in other Microdontinae. In these cases, the integument between sternites 1 and 2 often is very wide too, and sternites 2 and 3 are often strongly arched.

147. Sternite 3, position relative to lateral margins of tergite 3: normal (0); covering lateral margins of tergite (1) (Fig. 66).
State 1 exists only in the male of *Kryptopyga pendulosa* Hull, in which the lateral margins of tergite 3 seemed to be 'tucked in' behind the margins of sternite 3.
148. Abdomen, male sternite 5, length: long (0), short (1). H&S # 105.
149. Abdomen, male sternite 5, position: preabdominal (0), postabdominal (1). H&S # 106.
150. Abdomen, male sternite 8: fenestrate (0), not fenestrate (1). H&S # 110.
151. Tergite 4, lateral view, position relative to preceding tergites: normal, making angle of less than 60° (0); perpendicular (1) (Fig. 67).
State 1 exists only in species of *Ceratophya* Wiedemann (in the sense of Cheng & Thompson 2008) and in *Kryptopyga pendulosa* Hull.
152. Tergites in female, posterior margins, degree of overlap: normal (0); strongly overlapping next tergite (1) (Fig. 67).

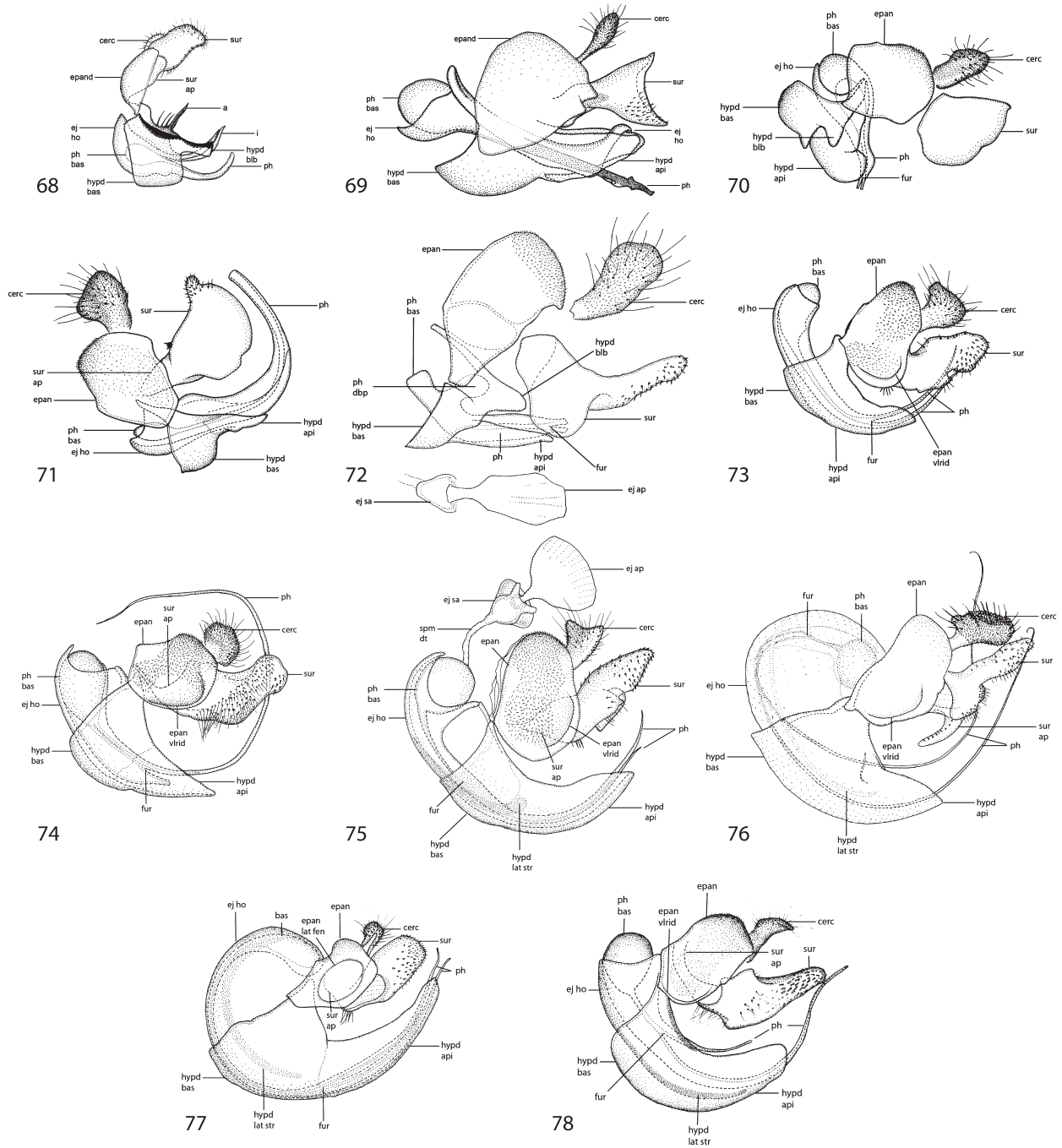

Figs. 68-78. Male genitalia, lateral view. (68) *Spheginobaccha macropoda*; (69) *Aristosyrphus primus*; (70) *Schizoceratomyia flavipes*; (71) *Stipomorpha maculipennis*; (72) *Archimicrodon ampefyanus*; (73) *Microdon carbonarius*; (74) *Omegasyrphus coarctatus*; (75) *Microdon mutabilis*; (76) *Microdon* (*Chymophila*) *aurifex*; (77) *Ubristes flavitibia*; (78) *Metadon bifasciatus*. Acronyms: a, accessory prong (sensu Thompson, 1974, only in *Spheginobaccha*); ph, phallus; ph ap, phallapodeme; ph bas, basal part of phallus; ph dbp, dorsobasal projection of phallus; cerc, cercus; ej ap, ejaculatory apodeme; ej ho, ejaculatory hood; ej sa, ejaculatory sac; epan, epandrium; epan lat fen, lateral fenestra of epandrium; epan vlrid, ventrolateral ridge of epandrium; fur, furcation point of phallus; hypd api, apical part of hypandrium; hypd bas, basal part of hypandrium; hypd blb, basolateral bulge of hypandrium; i, inner prong of ejaculatory hood (sensu Thompson, 1974, only in *Spheginobaccha*); spm dt, sperm duct; sur, surstylus; sur ap, surstylar apodeme.

Strongly overlapping tergites in the female possibly indicate that the abdomen can be extended telescopically, e.g. during oviposition. As for # 184, state 1 was found only in species of *Ceratophya* Wiedemann, 1830 and in *Kryptopyga pendulosa* Hull. These characters probably are strongly correlated, thus only # 184 was used in the analyses.

153. Abdomen, female abdominal segment 6, position: preabdominal (0), postabdominal (1). H&S # 114.
154. Abdomen, female, ovipositor, sclerotization: not sclerotized (0), sclerotized (1). H&S # 117.

Male genitalia

155. Superior lobe or paramere: fused to sternite (0), articulated with sternite (1), absent (2). H&S # 111.

State 2 was added to accommodate the absence of distinguishable parameres in Microdontinae.

156. Superior lobe, ctenidion: absent (0), present (1). H&S # 112.
157. Phallapodeme, development of: absent or much reduced (0) (Figs 68–80), long, laterally flattened (1) (Fig. 81). H&S # 113.

In Microdontinae, a phallapodeme was found only in *Spheginobaccha dexioides* Hull and *S. guttula* Dirickx (see Discussion).

158. Phallus, direction of curving: bent dorsad (0) (Figs 68, 71–78); straight or bent slightly ventrad (1) (Figs 69, 70).
159. Phallus, articulation point with hypandrium, position: basal (0) (Figs 68–80, apical (1) (Fig. 81).

In Eristalinae and Syrphinae the phallus articulates with the apical hypandrium, whereas in almost all Microdontinae articulation is basal. The only microdontine exception is the African taxon *Spheginobaccha guttula* Dirickx in which the articulation point is apical. In the Oriental species of *Spheginobaccha* articulation is basal, as in other Microdontinae.

160. Ejaculatory apodeme, degree of sclerotization: not sclerotized (0); sclerotized (1).

An unsclerotized ejaculatory apodeme was found only in *Paragodon* Thompson.

161. Ejaculatory sac, degree of sclerotization: not sclerotized (0); sclerotized (1)

An unsclerotized ejaculatory sac was found only in *Paragodon* Thompson and *Surimyia* Reemer.

162. Phallus, furcation: furcate (0) (Figs 70, 72–77); not furcate (1) (Figs 68, 69, 71).

Among Syrphidae, a furcate phallus is only known in Microdontinae. If the phallus is furcate, it is always split into dorsal and ventral processes; both seem connected to the sperm duct but no function is known.

163. Phallus, point of furcation: closer to base (0) (Figs 75, 76); halfway or closer to apex (1) (Figs 70, 72–74).
164. Phallus, length of processes relative to each other: about equally long or dorsal process little longer than ventral process (0) (Figs 70, 72, 73, 75–77); dorsal process $> 2\times$ length of ventral process (1) (Fig. 74); ventral process $> 2\times$ length of dorsal process (2) (Fig. 78).

This character applies only to taxa with a furcate phallus.

165. Phallus, length relative to apex of hypandrium: projecting not or little beyond apex of hypandrium (0) (Figs 69, 70, 72, 77); projecting far beyond apex of hypandrium (1) (Figs 71, 73–76).
166. Phallus, base, shape: not spherical (0) (Figs 72, 81); spherical (1) (Figs 68–71, 73–78, 80).

In most Microdontinae, the base of the phallus is formed by a spherical structure, to which the ejaculatory sac is connected through the sperm duct. This structure, named 'chitinous box' by Metcalf (1921), seems homologous to the basiphallus of McAlpine (1981) and Sinclair (2000).

167. Ejaculatory hood, dorsobasal projection, presence: absent (0) (Figs 68–71, 73–81); present (1) (Fig. 72).

In certain taxa, the basal part of the ejaculatory hood is strongly produced dorsomedially.

168. Hypandrium, apical part, separate lobes: absent (0) (Figs 70–77); present (1) (Figs 68, 69, 79, 80).

In most Microdontinae, the 'shaft' surrounding the phallus seems to comprise basal and apical parts. Although this distinction may be very clear (Figs 70–72), the parts may be smoothly fused (Figs 74–77), but the apical part usually is less sclerotized than the basal part and it is covered with very fine microtrichia, whereas on the basal part these are lacking. The basal part undoubtedly is the actual hypandrium, because it articulates with the epandrium basolaterally. Possibly, the apical part is homologous to the gonopods of other Diptera, which are usually simple in Muscomorpha and more or less absent in Syrphoidea (McAlpine 1981). In most Microdontinae the apical part consists of one single structure. If this structure is homologous to the gonopods indeed, then this would mean that the gonopods became fused. In a few taxa, the apical part of the hypandrium consists of two separate lobes, e.g. in *Aristosyrphus* (incl. *Eurypterosyrphus*), *Mixogaster* and *Spheginobaccha* (Figs 79–81), implying, perhaps, homology to gonopods.

169. Hypandrium, base, shape: not bulb-like (0) (Figs 73–77); bulb-like (1) (Figs 70–72).

The basal part of the hypandrium (the actual hypandrium; see # 200 for explanation) is considered bulb-like in shape when – in lateral view – its ventral side is clearly more convex than the apical part of the hypandrium (the presumed fused gonopods).

170. Hypandrium, basolateral bulges or projections: absent (0) (Figs 71, 73–77); present (1) (Figs 70, 72).
171. Hypandrium, 'lateral strips', presence: absent (0) (Figs 68–74); present (1) (Figs 75–77).

In certain taxa, dark lines are visible on both sides of the basal part of the ejaculatory hood, which continue on the basal part of the hypandrium, in which they seem to be embedded. These 'lateral strips' are labelled as 'aedeagal apodeme' by Vockeroth & Thompson (1987). This seems

unlikely, however, as the aedeagal apodeme is a single structure, whereas these 'lateral strips' are paired.

172. Epandrium, fenestrae, presence: absent (0) (Figs 68–76, 78–80); present (1) (Fig. 77).
The term 'fenestrae' indicates well-delimited, oval pits on both sides of the hypandrium. State 1 was found only in *Ubristes flavitibia* Walker.
173. Epandrium, ventrolateral ridges, presence: absent (0) (Figs 68–72); present (1) (Figs 73–78).

In several taxa, the hypandrium is depressed laterally, and the lateral depressions are delimited ventrally by a sharp ridge. The ridge may be very close to hypandrial margins and may be overlooked.

PCR amplification and obtained sequences

Table S1 indicates which fragments could be amplified for each sample. Total success rates for the different fragments were as follows: *COIa* - (89%); *COIb* (84%); *18Sa* (99%); *18Sb* (69%); *28S* (69%).

Phylogenetic analyses

Analyses of the the molecular dataset under parsimony resulted in 22 most parsimonious trees of length 8662 (strict consensus in Figure S1) and under Bayesian gave the tree in Figure S2.

Analyses of combined molecular and morphological datasets under parsimony resulted in three most parsimonious trees of length 9965 (strict consensus in Fig. 82) and under Bayesian gave the tree in Fig. 83.

Parsimony search of the morphological dataset for the total set of 189 taxa yielded 11 trees for the different k-values, four of which were used to construct a strict consensus (Figure S3).

Discussion

Evaluation of trees

The two trees based on the analyses of molecular data alone (strict consensus parsimony and Bayesian) are poorly resolved (Figures S1, S2). Most taxa are resolved within a large polytomy of Microdontinae, in which only a few small clades are recovered. In both trees, the Microdontinae are placed as sister group of other Syrphidae, and *Spheginobaccha* is placed as sister to the other Microdontinae, with high support. Otherwise, there are few corresponding nodes and most support values are low.

The addition of morphological characters to the dataset clearly adds much resolution to the trees (Figs 82, 83). Support remains generally low for the deeper nodes, but many more derived nodes have higher values. Again, Microdontinae are recovered as sister group of other Syrphidae, and *Spheginobaccha* is placed as sister to all other Microdontinae.

Following the reasoning of Kluge (1989) concerning the philosophy of total evidence in phylogenetic analyses, the results obtained from a combination of morphological and molecular data are preferred to those from a single data source. Therefore, the trees based on combined analyses (Figs 82, 83) were chosen as preferred results. However, several genus groups are not represented in combined analyses because of absence of molecular data. Thus, an analysis of morphology alone is presented here. This analysis includes 189 taxa, representing all genera and species groups as recognized by Reemer & Ståhls (2013) (Figure S3). The phylogenetic position of taxa which could not be included in combined analyses will be discussed based on these results.

Family affairs

Our results support the sister-group relationship of Microdontinae and other Syrphidae, as proposed originally by Thompson (1969) and subsequently by others (Skevington & Yeates, 2000; Ståhls *et al.*, 2003; Hippa & Ståhls, 2005; Rotheray & Gilbert, 2008). Our results are based on a wide representation of taxa: representatives of all valid genus groups are included, as well as taxa from all major biogeographic regions. In addition, both character sets (molecular and morphological) are larger than in previous analyses and the results can be regarded as additional support for this sister-group relationship. However, the results cannot be regarded as compelling evidence as analyses were not designed to test this relationship explicitly. For that, a much larger set of Syrphidae taxa would be necessary and preferably more taxa of related groups of 'lower Cyclorrhapha' included, such as Phoridae and Platypezidae.

According to Speight (2010) the presumed sister-group relationship between Microdontinae and other Syrphidae 'more-or-less reduces the issue of the correct placement of *Microdon* and allied genera to a matter of personal preference'. We advocate, however, that in this case, in which available evidence does not demand that the classification be changed, a conservative attitude is preferable.

Family group names

Two tribes are recognized within the Microdontinae: Spheginobacchini Thompson, 1972, which includes only the genus *Spheginobaccha*, and Microdontini Rondani, 1845 including all remaining taxa (Cheng & Thompson, 2008). The only other proposed family group names are Masarygidae of Brèthes (1908) and Ceratophyini of Hull (1949), unused since their introduction. Hull (1949) wrote: 'Perhaps two tribes should be recognized. The first would be the Microdonini distinguished by (. . .), and secondly the Ceratophyani (. . .).' Sabrosky (1999) argued that this name is unavailable, as it was mentioned only casually within a short diagnosis of a group, not as a formal proposal of a new group name. However, this can be regarded as a 'conditional proposal' of a new name: as

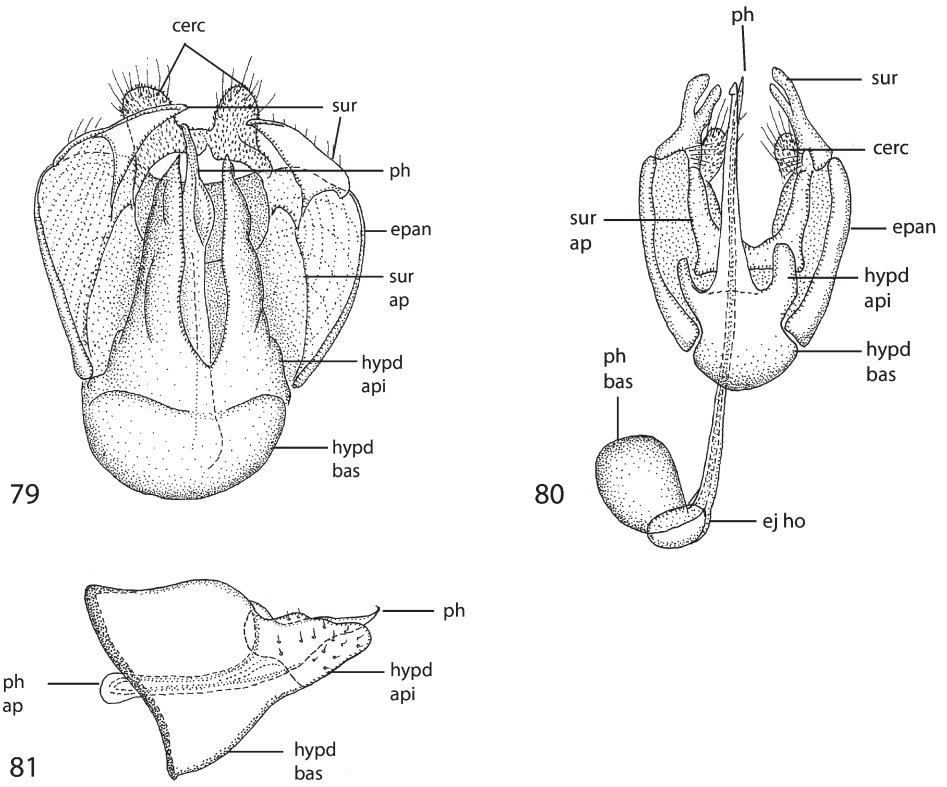

Figs. 79-81. Male genitalia, ventral view. (79) *Mixogaster breviventris*; (80) *Eurypterosyrphus* cf. *melanopterus*; (81) *Spheginobaccha guttula*, hypandrium and phallus, lateral view.

published before 1961, there is no reason for considering this name unavailable (ICZN, 1999: art. 15.1).

Recognition of additional tribes could make the group more 'manageable' in taxonomic, biogeographical and evolutionary studies and discussions. However, for introducing new family group names (or changing the status of available ones), we feel that the clades under consideration should be sufficiently 'reliable'. Our support values (Figs 84, 85) aid in assessing clade reliability. For most larger clades, these values are low, but smaller clades for which these values are higher, are here – subjectively – considered to be of generic level, rather than of family-group level. Because of this, and also because of the considerations on missing data as discussed in the previous paragraph, the introduction of new tribal names or reinstating available family group names based on the present phylogenetic hypotheses is deemed unjustified.

Intra- and infrageneric relationships

Several smaller clades have high support and stability values, and indicate affinities between genus and species groups that have not been suggested previously. We address these affinities, and discuss the classification of Reemer & Ståhls (2013).

Afromicrodon. This genus is recovered at an early node in all trees, but at varying positions. However, support values are quite low, so the position is not clarified.

Archimicrodon. In combined analyses, two of the three groups recognized by Reemer & Ståhls (2013) are represented: *Hovamicrodon* (unidentified species) and *Archimicrodon* s.l. (*clatratus* and *simplex*). These taxa were recovered as a clade. The analysis based on morphological characters also includes two species of *Archimicrodon* s.s.: *A. malukensis* sp.n. and *A. simplicicornis*. These species are united in a clade within a large polytomous clade, which offers no hypothesis as to the relationships with *Archimicrodon* s.l. and *Hovamicrodon*.

The three groups are very similar in morphology, and are likely to be closely related. The subgenus *Hovamicrodon* probably is monophyletic, considering the spatulate scutellar calcars and distribution restricted to Madagascar. However, as the phylogenetic results indicate, it is so closely related to *Archimicrodon* s.l. (which is recovered as paraphyletic with respect to *Hovamicrodon*) that separate generic status seems unwarranted. Besides, a spatulate shape of the scutellar calcars can be found also in certain species of the New World groups *Laetodon* and *Serichlamys*. The latter genus is recovered as sister to *Archimicrodon* in combined analyses. As this

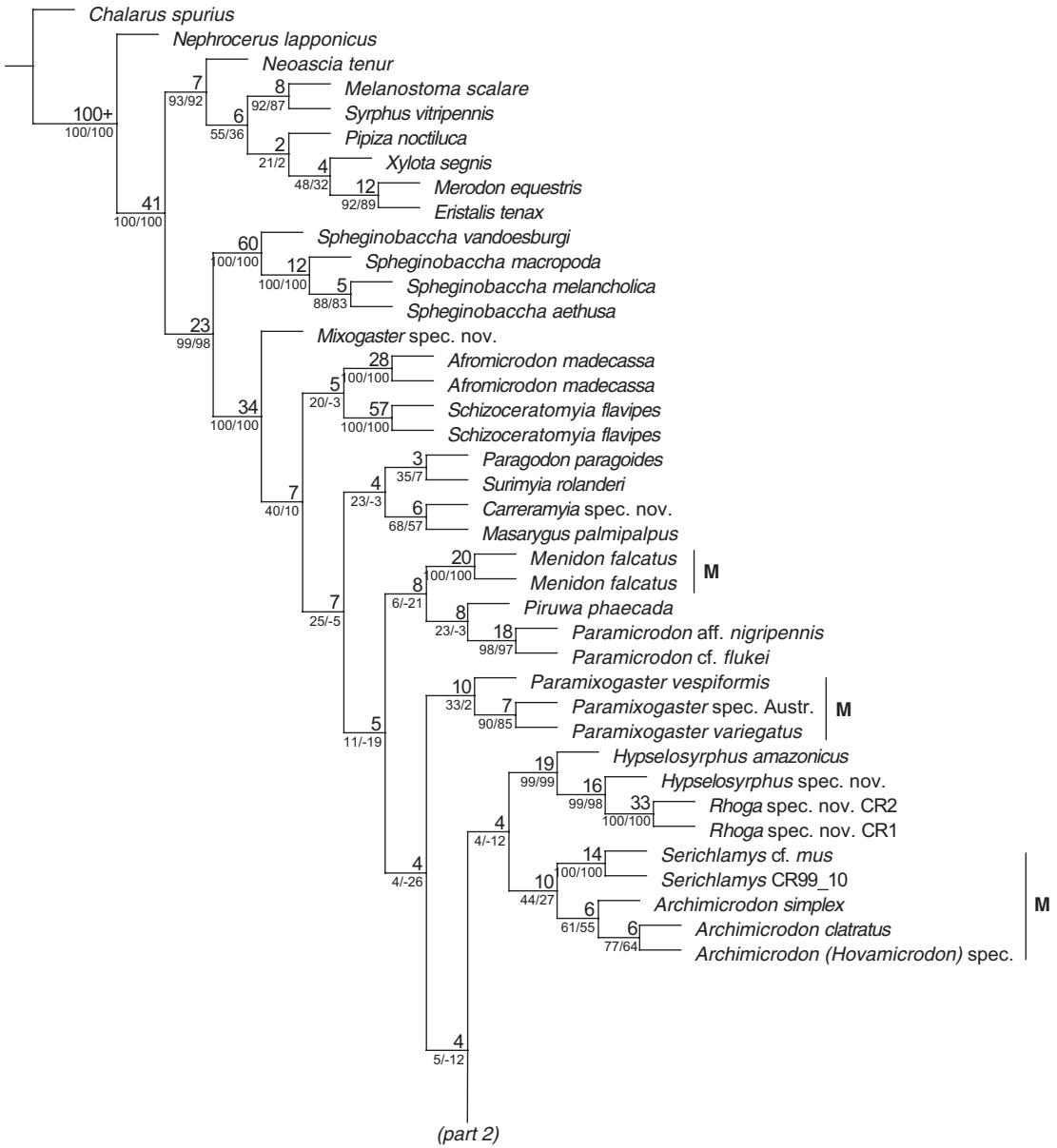

Fig. 82a. Parsimony analysis of combined molecular and morphological data: strict consensus of three trees of length 9965. Values above branch indicate Bremer support, below branch Jackknife values/GC frequency differences. Vertical lines marked 'M' indicate taxa included in the genus *Microdon* by previous authors.

character is not unique, it provides insufficient basis on which to base a genus.

Aristosyrphus. No molecular data available. In morphological analyses the subgenera *Aristosyrphus* and *Eurypterosyrphus* are recovered as sister groups. This does not contradict the present rank of *Eurypterosyrphus* as subgenus of *Aristosyrphus* (Cheng and Thompson, 2008; Reemer & Ståhls, 2013). Considering the large morphological variation within this genus, especially within the subgenus *Eurypterosyrphus*, both in external characters and male genitalia, the phylogenetic relationships of these taxa need to be examined in more detail, preferably with the aid of molecular characters.

Although *Aristosyrphus* and *Mixogaster* were not recovered as closely related groups, certain morphological characters in common to these taxa may suggest a closer relationship. For instance, in some specimens of *Aristosyrphus primus* an anterior stump is present at vein M (Fig. 48). This character always has been diagnostic for *Mixogaster* (Hull, 1954; Cheng & Thompson, 2008). A facial tubercle similar to that of *Eurypterosyrphus* is present also in certain species of *Mixogaster*. In addition, the genera share an unfurcate

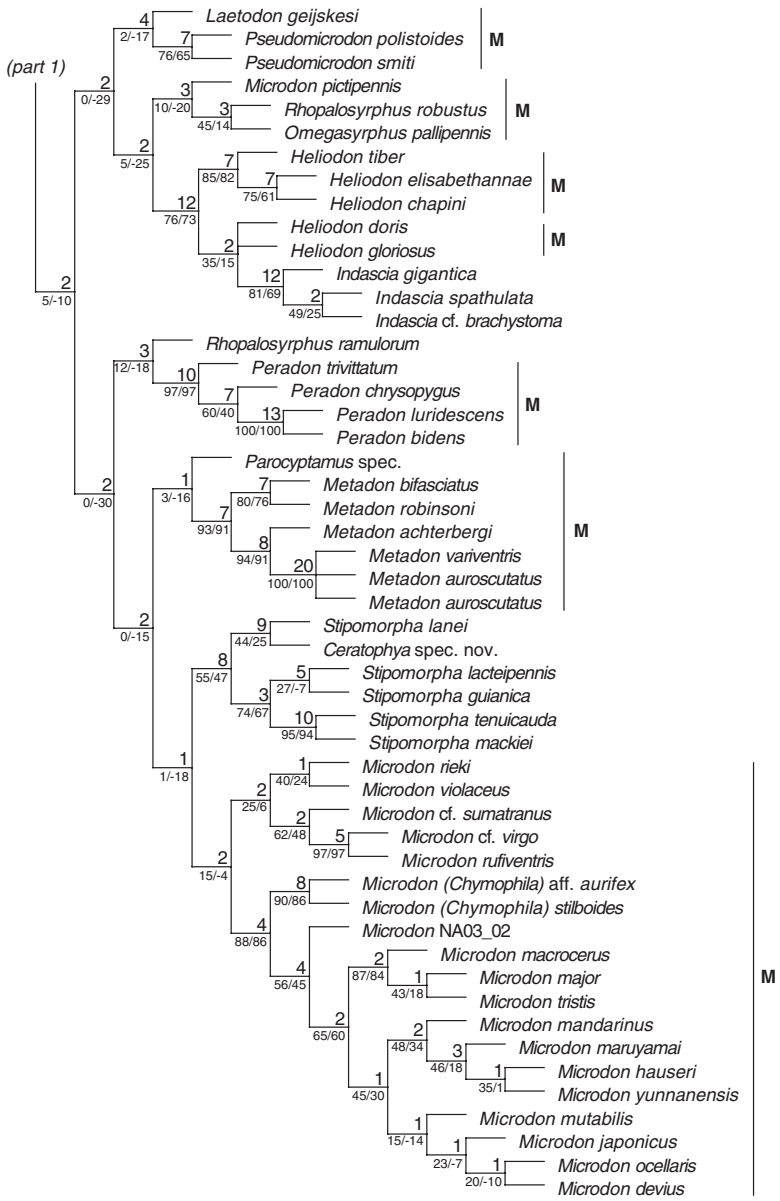

Fig. 82b. Continued

phallus and the apical part of the hypandrium consisting of two separate lobes (ventral view). The latter character occurs also in *Paramicrodon* and *Spheginobaccha*.

Bardistopus. No molecular data available. In morphological analysis *Bardistopus* is placed as sister to a clade containing several taxa in which the males have a bifurcate basoflagellomere: *Schizoceratomyia*, *Furcantenna* and *Carreramyia*. In *Bardistopus* the basoflagellomere is not furcate. Tentatively, a placement with *Paramixogaster* seems more plausible, because these taxa share the following characters: basoflagellomere much longer than scape, not furcate; postpronotum bare; vein R4 + 5 with posterior appendix; phallus strongly bent dorsad, relatively deeply furcate. Unlike *Paramixogaster* the abdomen is not constricted in dorsal view, but tergite 2 in lateral view clearly is flattened relative to tergites 3 and 4.

Carreramyia. Carreramyia megacephalus is one of the microdontine taxa in which the basoflagellomere of the male is bifurcate. When Shannon (1925) described this species, he attributed it to *Microdon*, denying the furcate antenna warranted erection of a new genus, as this condition is restricted to the male. van Doesburg (1966) did not agree and considered *Microdon megacephalus* to be very different from other Neotropical taxa with furcate basoflagellomeres (*Masarygus* and *Schizoceratomyia*), and hence erected for it the genus *Carreramyia*. Cheng & Thompson (2008) considered *Carreramyia megacephalus* as a *Ubristes* species with furcate basoflagellomere, a character they considered

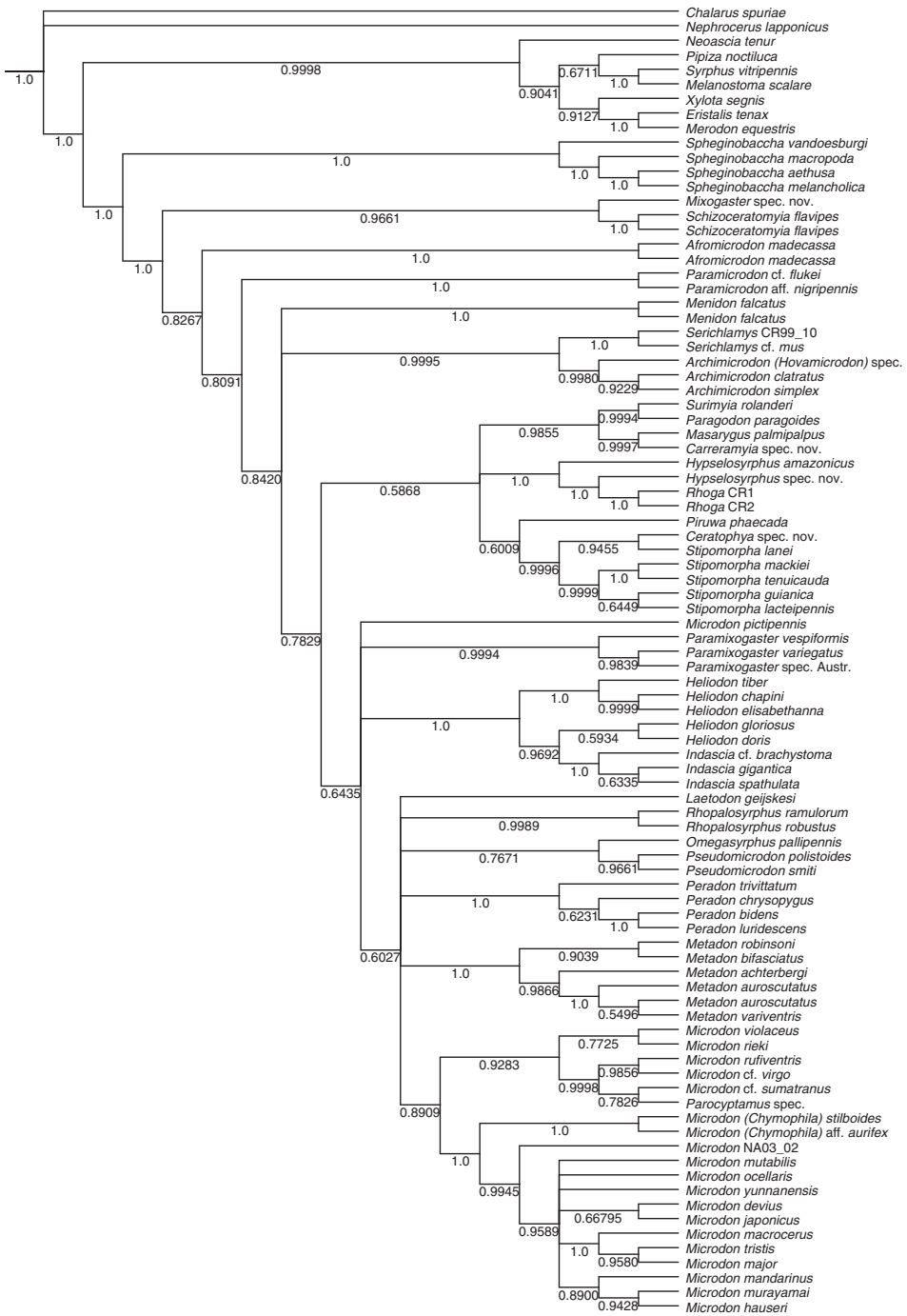

Fig. 83. Results of Bayesian analysis of combined molecular and morphological data. Values indicate Bayesian probability (> 50%).

to be of subgeneric value only. The phylogenetic results indicate that this taxon is unrelated to *Ubristes* (q.v.), nor is it related to any of the other groups synonymized previously with *Ubristes* (*Hypselosyrphus* and *Stipomorpha*). Combined analysis placed *Carreramyia* in a clade with *Masarygus*, with moderate support. As there are clear morphological differences between these two taxa (Reemer & Ståhls, 2013), we do not propose synonymy.

Ceratophya. In combined analyses, *Ceratophya* sp. was placed within *Stipomorpha*, as follows: [(*C*. sp. nov. + *S. lanei*) + (other *Stipomorpha* species)]. However, there are several important morphological differences between *Ceratophya*

and *Stipomorpha* (e.g. tergites 3–4 fused vs. not fused, sternites 2–3 widely separated vs. narrowly separated, phallus furcate vs. unfurcate). It seems wise to wait with making changes in the taxonomy of these genera until more species can be included in the molecular dataset.

Ceriomicrodon. Based on morphology alone, this taxon was placed in the clade also comprising *Domodon*, *Pseudomicrodon* and *Rhopalosyrphus*. In male genitalia, *Ceriomicrodon* is very similar to these taxa, having in common a strongly elongate, whip-like dorsal process of the phallus. It resembles *Rhopalosyrphus* in the ventrally bulging face, the antennal fossa being wider than high, the narrow area of enlarged ommatidia on the eye, and the constricted abdomen. The bare postpronotum and bare katepimeron distinguish *Ceriomicrodon* from *Rhopalosyrphus*, whereas the bare postpronotum and the flat vertex distinguish it from *Pseudomicrodon*.

Cervicorniphora. Morphological analysis provided few clues as to the taxonomic affinities of this taxon, although it seems unrelated to other taxa in which the male has a furcate basoflagellomere.

Chrysidimyia. Morphological analysis placed *Chrysidimyia* in a large polytomy, leaving its phylogenetic affinities unresolved. As Reemer & Ståhls (2013) argue, the male genitalia of *Chrysidimyia* resemble those of *Laetodon*; these taxa share an unfurcate phallus and a long posterior process on the phallus. These taxa also have in common metallic body coloration and pilose eyes.

Chymophila (subgenus of Microdon). Combined analyses included one Oriental and one Neotropical species, which are recovered as sister species within *Microdon*.

Dimeraspis (subgenus of Microdon). Morphological analysis includes three species belonging to this taxon (*M. abditus, M. fuscipennis, M. globosus*), but the results offer little clues as to their relationships. Because of similarities in male genitalia this group might be related to *Archimicrodon, Menidon* or *Serichlamys*, but is continued to be treated as subgenus of *Microdon*.

Domodon. No molecular data are available. Morphological analysis placed *Domodon* in a clade with *Ceriomicrodon*, *Omegasyrphus*, *Pseudomicrodon* and *Rhopalosyrphus*. These genera have in common a strongly elongate, whip-like dorsal process of the phallus.

Furcantenna. Based on morphology, *Furcantenna nepalensis* was recovered in a clade containing *Carreramyia* and *Schizoceratomyia*. *Furcantenna* is very similar to *Schizoceratomyia* in both external morphology and male genitalia, but presently available evidence is not conclusive about the exact relationships between these taxa.

Heliodon. Five species of *Heliodon* are included in combined analyses. These are recovered in a clade containing also *Indascia*; thus, *Heliodon* appears as paraphyletic with respect to that genus. However, support for the subclade containing the *Indascia* species is low. As *Heliodon* morphology is distinct from that of *Indascia* (Reemer & Ståhls, 2013), these taxa will continue to be considered as separate.

Hypselosyrphus. In combined analyses (Figs 82, 83), *Hypselosyrphus* was recovered in a clade together with *Rhoga*, with high support. *Hypselosyrphus* is paraphyletic with respect to *Rhoga*, as seen in morphological analyses. However, morphological variation within *Hypselosyrphus* is large, which could indicate a more complicated phylogeny so *Hypselosyrphus* and *Rhoga* are retained as separate genera.

Indascia. Three species of *Indascia* are included in combined analyses: these are recovered in a well-supported clade, part of a larger clade containing also *Heliodon*, which appears paraphyletic with respect to *Indascia*. However, support values are low, and as *Indascia* is distinct from *Heliodon* in morphology, these taxa are considered separate genera.

Superficially, species of *Indascia* look similar to those of *Paramicrodon* (as noticed by Cheng & Thompson, 2008), but available phylogenetic evidence provides no support for a close relationship. See *Paramixogaster* for further discussion.

Kryptopyga. Morphology provides no evidence for a close relationship with *Ptilobactrum*; *Kryptopyga pendulosa* is placed as sister of *Ceratrichomyia*. These taxa share the pilose basoflagellomere in the male, the swollen vertex and dorsal occiput, and the unfused tergites 3 and 4. Male genitalia are quite different, and in *Kryptopyga* the mesonotal transverse suture is incomplete.

Laetodon. The included species (Reemer & Ståhls, 2013) were placed previously in *Microdon* (Thompson, 1981). In combined analyses, *Laetodon geijskesi* (Doesburg) is placed quite distant from *Microdon*. The analysis of morphology alone includes an additional species, *L. laetus* (Loew), but provides no alternative hypothesis as to the relationship with *Microdon*. See *Chrysidimyia* for further discussion.

Masarygus. Because no fresh specimens of the type species of *Masarygus*, *M. planifrons*, were available, *M. palmipalpus* Reemer was substituted. Morphological analysis placed the two species as sister taxa, but in combined analysis, *M. palmipalpus* was placed as sister of *Carreramyia tigrina*, with moderate support. The clade including both taxa was placed as sister of (*Paragodon* + *Surimyia*), with low support.

Two undescribed species belonging to this genus are included in morphological analysis under *Masarygus* sp. 1 and sp 2 (Reemer & Ståhls, 2013). Whereas sp. 1 is placed in the same clade as *M. planifrons* and *M. palmipalpus*, the relationships of sp. 2 are unresolved.

Megodon (subgenus of Microdon). Megodon stuckenbergi was included in the analysis of morphological characters, which recovered it within a clade also containing *Microdon* s.s. Exact relationships, however, remain unclear.

Menidon. Combined analysis places *Menidon falcatus* in a clade with *Paramicrodon* and *Piruwa*, but support values for this clade are low. Neither Bayesian analysis nor parsimony analysis based on morphology alone offers an alternative solution.

Mermerizon. In morphological analysis, *Mermerizon inbio* is recovered in a clade containing no others. Similar taxa which also mimic stingless bees, e.g. *Hypselosyrphus*, *Rhoga*, *Stipomorpha*, *Surimyia*, are placed in different clades.

Metadon. In combined analyses, the included species of *Metadon* are grouped in a clade with high support. Relationships with other genera are less clear: in combined parsimony analysis, *Metadon* is recovered as sister of *Parocyptamus*, within a clade containing also *Microdon* s.s., *Stipomorpha* and *Ceratophya*. Bayesian analysis places it in a polytomy with *Laetodon*, *Microdon*, *Omegasyrphus*, *Parocyptamus*, *Pseudomicrodon* and *Rhopalosyrphus*. The analysis of morphology alone includes a larger number of species (also from Africa), and *Metadon* is placed as sister group of *Heliodon*, within a clade containing *Ceriomicrodon*, *Domodon*, *Omegasyrphus*, *Peradon*, *Pseudomicrodon* and *Rhopalosyrphus*.

Microdon. Microdon has served as a 'waste basket' for taxa of which taxonomic affinities were inadequate for location elsewhere. Although several taxa were assigned to other genera, subsequent authors have considered those genera as subgenera of *Microdon*. The present analyses contain many species formerly placed in *Microdon*. As can be seen in Fig. 82 (taxa classified previously in *Microdon*, or representatives of these taxa, are indicated with an 'M') this group is polyphyletic and its representatives are scattered over different parts of the tree. Although the exact positions of these groups may change in future analyses when more taxa and more molecular data are included, these results provide sufficient basis for subdividing *Microdon* into different monophyletic units (Reemer & Ståhls, 2013). For several species which could be included only in the analysis of morphological characters, however, phylogenetic affinities remain obscure (Figure S3). These taxa will be maintained in *Microdon* s.l. until better phylogenetic hypotheses are available.

Mixogaster. According to combined analysis and morphology alone, *Mixogaster* is the first branch within the tribe Microdontini, with high support. Bayesian analysis recovers (*Mixogaster* + *Schizoceratomyia*) as the first branch within the Microdontini. Analyses of molecular data alone recover *Mixogaster* in shallower positions. Interestingly, the most important diagnostic character of *Mixogaster*, the anterior appendix of vein M, is found also in *Spheginobaccha* and certain specimens of *Aristosyrphus primus*. These taxa also share the character of the apical part of the hypandrium consisting of two separate lobes. No close relationship between *Mixogaster* and *Aristosyrphus* was recovered by the analysis of morphological characters (Figure S3), but see *Aristosyrphus* (q.v.).

Myiacerapis (subgenus of Microdon). No molecular data available. Morphology placed *Myiacerapis* in an unresolved clade containing several (sub)genera, such as *Metadon, Microdon* s.s., *Parocyptamus*, *Ubristes*. Its phylogenetic affinities remain unclear.

Oligeriops. No molecular data available. Morphology does not resolve affinities of *Oligeriops dimorphon* (Ferguson).

Omegasyrphus. Combined analysis places *Omegasyrphus pallipennis* Curran as sister of *Rhopalosyrphus robustus*, with low support. In Bayesian analysis of combined characters, *O. pallipennis* was placed as sister to *Pseudomicrodon*. *Omegasyrphus*, *Pseudomicrodon* and *Rhopalosyrphus* are similar in the structure of the phallus and the shape of the surstylus (Reemer & Ståhls, 2013). These are shared with *Ceriomicrodon* and *Domodon*. Even though the results of the analyses only partly support the monophyly of a clade containing these taxa, the characters of the male genitalia suggest they are related.

Paragodon. Thompson (1969) in describing this genus, stated that it appeared to be the 'most primitive' microdontine fly known. In both analyses of combined molecular and morphological characters, *Paragodon* is not placed in such a position, albeit at a relatively early node, with low support in parsimony analysis. Additional sampling of molecular characters of other taxa in the basal part of the tree will be needed. *Paragodon* was recovered as sister to *Surimyia*.

Paramicrodon. In all analyses presented here, except parsimony molecular analysis, the Neotropical *Paramicrodon* cf. *flukei* and the Oriental *P*. aff. *nigripennis* were placed together in a well-supported clade. In the analysis based on morphology three additional species (two Neotropical, one Oriental) are also resolved in a clade with the other species. No doubt the Neotropical and Oriental species belong in the same genus. Further relationships remain uncertain, and the phylogenies presented here are contradictory.

Paramixogaster. Three species of this genus included in the analyses of combined molecular and morphological characters are recovered as a monophyletic. A larger number of species was included in morphological analysis. The resulting phylogeny supports the inclusion of the following Afrotropical species in this genus, which considered previously to be Oriental and Australian in its distribution: *Microdon acantholepidis*

Speiser, *Microdon crematogastri* Speiser, *Microdon illucens* Bezzi, *Pseudomicrodon elisabethae* Keiser. *Paramixogaster* sp. from Madagascar is also added to this genus. Morphological analysis also recovered *Ptilobactrum* (q.v.) within *Paramixogaster*.

Parocyptamus. Parocyptamus is recovered in contradictory positions: combined parsimony analysis placed it as sister group to *Metadon*, whereas Bayesian analysis placed it within *Microdon* s.l. Parsimony analysis of morphology places it in a clade with three species of *Microdon* s.l.

Peradon. Peradon bidens and *P. luridescens* (*bidens*-group), *P. chrysopygus* (*flavofascium*-group) and *P. trivittatus* (*trivittatus* group) are recovered as monophyletic with high support. Analysis of morphology alone recovers additional species *P. flavofascium* in the same clade.

Most assigned species were included in *Microdon* in the most recent classification of Neotropical Microdontinae (Thompson *et al.*, 1976), but here this group is not recovered as part of or sister to *Microdon*.

Piruwa. In combined analysis, this taxon was placed as sister to *Paramicrodon* with low support. Bayesian analysis of combined characters places it as sister to the clade containing *Ceratophya* and *Stipomorpha*.

Pseudomicrodon. The two species of *Pseudomicrodon* included in combined analyses are placed together in both analyses, but as sister to *Omegasyrphus pallipennis* in Bayesian analysis and as sister to *Laetodon geijskesi* in parsimony analysis (low support). In morphological analyses, *Pseudomicrodon* species are placed in a clade with *Ceriomicrodon*, *Domodon*, *Omegasyrphus* and *Rhopalosyrphus*, and *Pseudomicrodon* does not appear as monophyletic. Phylogenetic affinities between these taxa are likely because of strong similarities in male genitalic morphology (phallus with dorsal process strongly elongated). At present, the morphological basis for distinguishing *Ceriomicrodon*, *Pseudomicrodon* and *Rhopalosyrphus* is narrow. The groups are most probably related, but it is doubtful whether they are monophyletic, considering morphological variation.

Ptilobactrum. In morphological analysis, *Ptilobactrum* is placed within *Paramixogaster* but differences are considered too large to alter the rank of *Ptilobactrum* to subgenus within *Paramixogaster*. For instance, in contrast with *Paramixogaster*, the basoflagellomere and postpronotum are pilose and the abdomen is oval. Phylogenetic affinities of *Ptilobactrum* can best be re-assessed when molecular data become available.

Rhoga. In the molecular and combined analyses, *Rhoga* is recovered within *Hypselosyrphus*, with high support, a result found also in the analysis based on morphology only, in which more species were included. *Hypselosyrphus* (q.v.) is paraphyletic with respect to *Rhoga*.

Rhopalosyrphus. In parsimony analyses (both of molecular and combined), the two included species of *Rhopalosyrphus* were placed in different clades. However, in both Bayesian analyses these were placed as sisters. Analysis of morphology includes five species, four of which are placed in a monophyletic clade. In morphological analysis, *Rhopalosyrphus* is recovered in a clade with *Ceriomicrodon, Domodon, Pseudomicrodon* and *Omegasyrphus*. Close affinities between these taxa are likely because of similar male genitalia (phallus with strongly elongated dorsal process).

Schizoceratomyia. Combined analyses included only one species, recovered in deep positions, but with different sister groups: *Afromicrodon, Mixogaster* or *Paramicrodon*. In analysis of morphology alone, it is placed in a clade also containing several other taxa with a furcate basoflagellomere in the male (*Carreramyia, Furcantenna, Masarygus*). As this grouping is lost when molecular characters are added, it appears that *Schizoceratomyia* cannot be treated as synonymous with *Masarygus*, as Hull (1949) and Papavero (1962) proposed. *Johnsoniodon malleri* Curran is placed within *Schizoceratomyia*, supporting its inclusion by Cheng & Thompson (2008) and Reemer & Ståhls (2013).

Serichlamys. Serichlamys differs from *Microdon* s.s. most in genital features: phallus furcate apically, hypandrium with bulb-like base, surstylus with long, ventrally directed lobe (Reemer & Ståhls, 2013). Its independent phylogenetic position from *Microdon* s.s. is confirmed by its sister-group relationship with *Archimicrodon*. The type species of *Serichlamys* (*S. rufipes*) and *S. scutifer* are not recovered with other *Serichlamys* in morphology analysis (but in a large polytomy), but the similarities in wing venation and male genitalia are considered great enough to classify all considered species in this genus.

Spheginobaccha. Hull (1949) was the first to include *Spheginobaccha* in the Microdontinae. Thompson (1969) excluded it, after which Ståhls *et al.* (2003) included it again based on a sister-group relationship of *Spheginobaccha* to all other Microdontinae, as recovered in combined analyses. All our analyses affirm *Spheginobaccha* as a sister to all other Microdontinae, with high support.

Thompson (1974) recognized three species groups: the Oriental *macropoda* group (*Spheginobaccha* s.s. in Cheng & Thompson, 2008), the African *rotundiceps* group (subgenus *Dexiosyrphus*) and the African *perialla*-group. Our results suggest that the *perialla* group (represented by *S. guttula* in the dataset) is sister to *rotundiceps* group + *macropoda* group, as noted by Thompson (1974).

Stipomorpha. Combined phylogenetic hypotheses placed *Ceratophya* sp. within *Stipomorpha*, as did Bayesian analysis of molecular data. Analysis of morphology alone, which includes additional species of *Ceratophya* and *Stipomorpha*, recovers both as monophyletic. Given several important morphological differences between *Stipomorpha* and *Ceratophya* (e.g. tergites 3–4 fused vs. not fused, sternites 2–3 widely separated or narrowly separated, phallus furcate or unfurcate), conclusions about the taxonomic status of these genera should await wider molecular data.

Sulcodon. No molecular data available. Morphology provides no clues on the affinities of this taxon, as it was placed in a large polytomy containing other species of *Microdon* as well as species of several other genera.

Surimyia. When *Surimyia* was described, a species assigned previously to *Paragodon* was included (*P. minutula* Doesburg). Several morphological characters indicate differences between these genera (Reemer, 2008). In both combined analyses, and also in Bayesian analysis of molecular data, *Paragodon* and *Surimyia* are recovered with low support as sister groups. However, fundamental morphological differences between the taxa (Reemer & Ståhls, 2013) suggest that, although closely related, they should be considered as separate genera.

Syrphipogon (subgenus of Microdon). Hull (1937) erected *Syrphipogon*, mentioning that it is related to *Microdon*. Steyskal (1953) referred to Hull's description in his own description of an apparently very similar species, but considered the differences from *Microdon* insufficient for generic status. Morphological analysis places *Syrphipogon fucatissimus* in an unresolved clade which also contains *Microdon* s.s., but provides no clues as to their relationships. In external characters and male genitalia these taxa are quite similar, and thus it seems justified to treat *Syrphipogon* as a subgenus of *Microdon*, as proposed by Reemer & Ståhls (2013).

Thompsodon. No molecular data available: known from one female specimen only, so the male genitalia are unknown. As these characters are important in morphological analysis, this genus was excluded from analysis.

Ubristes. Thompson *et al.* (1976) included in *Ubristes* the type species of *Carreramyia*, *Hypselosyrphus* and *Stipomorpha*. The latter two groups were considered as 'subgroups' of *Ubristes* by Cheng & Thompson (2008). Based on morphology alone, *Ubristes flavitibia* was placed in an unresolved clade with (amongst others) *Microdon* s.s., but to the exclusion of *Carreramyia*, *Hypselosyrphus* and *Stipomorpha*, supporting Reemer & Ståhls (2013) treatment of these taxa as separate genera.

Undescribed genus #1. No molecular data available: for morphology, see Reemer & Ståhls (2013). Morphological analysis provides no indication of relationships.

Undescribed genus #2. No molecular data available: for morphology see Reemer & Ståhls (2013). In morphological analysis, this taxon is placed in a clade which contains other genera with a furcate male basoflagellomere (*Carreramyia*, *Furcantenna*, *Masarygus*, *Schizoceratomyia*). However, these genera are not recovered in a clade in combined analyses, so whether 'Undescribed genus #2' relates to any remains to be seen.

Concluding remarks

Our phylogenetic trees contain many poorly supported nodes and contradict each other on many points. Obviously, this is not the 'final word' concerning phylogenetic relationships of Microdontinae taxa. In our molecular dataset, only 28 of the 43 genera recognized by Reemer & Ståhls (2013) could be included, and more should be sought. More resolution can be expected also with increased taxon sampling within heterogenous genera, especially because such genera are mainly found in the deeper parts of the tree (e.g. *Aristosyrphus*, *Mixogaster* and *Schizoceratomyia*).

Despite the shortcomings, certain clades were recovered in both analyses (parsimony and Bayesian) of combined molecular and morphological characters (Table S5), most with high support, and thus form robust hypotheses. Both analyses agree also in the relatively early branching positions of *Mixogaster*, *Schizoceratomyia*, *Afromicrodon* and *Paramicrodon*.

Supporting Information

Additional Supporting Information may be found in the online version of this article under the DOI reference: 10.1111/syen.12020

Table S1. List of voucher specimens used for morphological and molecular data matrices.

Table S2. List of primers used for DNA amplification.

Table S3. Results of evaluations of all trees obtained with parsimony analysis of morphological characters under implied weighting for the total set of 189 taxa.

Table S4. Morphological character states matrix for all examined taxa.

Table S5. Clades recovered by both (parsimony and Bayesian) combined analyses of morphological and molecular characters, with support values.

Figure S1. Parsimony analysis of molecular data: strict consensus of 22 most parsimonious trees of length 8662. Values above branch indicate Bremer support, below branch Jackknife values/GC frequency differences.

Figure S2. Results of Bayesian analysis of molecular data. Values indicate Bayesian probability (> 50%).

Figure S3. Strict consensus of four trees found under implied weighting for four *k*-values (corresponding with character fits 0.62, 0.66, 0.70 and 0.74) for the total set of 189 taxa.

Acknowledgements

Most species of Microdontinae are collected rarely, so we are greatly indebted to all entomologists who have so generously provided us with material, either from their personal collections or from those of their institutions: Kees van Achterberg (RMNH), Brian V. Brown, Ben Brugge (ZMAN), Daniel Burckhardt (NMB), Jean A. Cerda, Christophe Daugeron (MNHN), K.-D. Dijkstra, Tim Faasen, Stephen Gaimari (CSCA), Aniel Gangadin, David A. Grimaldi (AMNH), Martin Hauser, Niklas Jönsson (NHRS), Stephen A. Marshall, Ximo Mengual, Frank Menzel (DEI), Burgert Muller (NMSA), Tam Nguyen (AMNH), Thomas Pape (ZMUC), Philip Perkins (MZC), Chris Raper, Peter Sehnal (NMW), Zoë Simmons (OUMNH), Jeff Skevington (CNC), John T. Smit, Villu Soon, Wouter van Steenis, Jens-Hermann Stuke, F. Christian Thompson (USNM), Rob de Vries (RMNH), Shaun Winterton, Nigel Wyatt (BMNH), S. Yoshimatsu (ITLJ), Chen Young (CM), Manuel Zumbado (INBIO).

Thanks to the skills and effort of Elvira Rättel (MZH) we amplified more DNA fragments than we could ever have done without her.

The first author thanks Kees van Achterberg for frequent access to his photographic and microscopic equipment. Special thanks are due to F. Christian Thompson for encouraging the first author to take up the work on this extraordinary group of flies, and for his many comments and advice.

References

Brèthes, J. (1908) Masarygidae. Una nueva familia de dípteros. *Anales del Museo Nacional de Buenos Aires, Series III*, **10**, 439–443.

Cheng, X.-Y. & Thompson, F.C. (2008) A generic conspectus of the Microdontinae (Diptera: Syrphidae) with the description of two new genera from Africa and China. *Zootaxa*, **1879**, 21–48.

van Doesburg, P.H. Sr. (1966) Syrphidae from Suriname. Additional records and descriptions. *Studies on the Fauna of Suriname and other Guyanas*, **9**, 61–107.

Goffe, E.R. (1952) An outline of a revised classification of the Syrphidae (Diptera) on phylogenetic lines. *Transactions of the Society for British Entomology*, **11**, 97–124.

Goloboff, P.A. (1993) Estimating character weight during tree search. *Cladistics*, **9**, 83–91.

Goloboff, P.A. (2008) Calculating SPR distances between trees. *Cladistics*, **24**, 591–597.

Goloboff, P.A., Farris, J., Källersjö, M., Oxelmann, B., Ramirez, M. & Szumik, C. (2003) Improvements to resampling measures of group support. *Cladistics*, **19**, 324–332.

Goloboff, P.A., Carpenter, J.M., Arias, J.S. & Esquivel, D.R.M. (2008a) Weighting against homoplasy improves phylogenetic analysis of morphological datasets. *Cladistics*, **24**, 758–773.

Goloboff, P.A., Farris, J.S. & Nixon, K.C. (2008b) TNT, a free program for phylogenetic analysis. *Cladistics*, **24**, 774–786.

Golubchik, T., Wise, M.J., Easteal, S. & Jermiin, L.J. (2007) Mind the gaps: evidence of bias in estimates of multiple sequence alignments. *Molecular Biology and Evolution*, **24**, 2433–2442.

Hippa, H. & Ståhls, G. (2005) Morphological characters of adult Syrphidae: descriptions and phylogenetic utility. *Acta Zoologica Fennica*, **215**, 1–72.

Huelsenbeck, J.P. & Ronquist, F. (2001) MrBayes: bayesian inference of phylogeny. *Bioinformatics*, **17**, 754–755.

Hull, F.M. (1937) A megamorphic and two curious mimetic flies. *Psyche*, **44**, 116–121.

Hull, F.M. (1949[publication states 1948]) The morphology and interrelationships of the genera of syrphid flies, recent and fossil. *Transactions of the Zoological Society of London*, **26**, 257–408.

Hull, F.M. (1954) The genus *Mixogaster* Macquart (Diptera, Syrphidae). *American Museum Novitates*, **1652**, 1–28.

ICZN [International Commission on Zoological Nomenclature] (1999) *International Code of Zoological Nomenclature*, 4th edn. The International Trust for Zoological Nomenclature, London.

Katoh, K. & Toh, H. (2008) Recent developments in the MAFFT multiple sequence alignment program. *Briefings in Bioinformatics*, **9**, 286–298.

Katoh, K., Misawa, K. & Kuma, K. (2002) MAFFT: a novel method for rapid multiple sequence alignment based on fast Fourier transform. *Nucleic Acids Research*, **30**, 3059–3066.

Katoh, K., Asimenos, G. & Toh, H. (2009) Multiple alignment of DNA sequences with MAFFT. *Methods in Molecular Biology*, **537**, 39–64.

Kluge, A.G. (1989) A concern for evidence and a phylogenetic hypothesis of relationships among Epicrates (Boidae, Serpentes). *Systematic Zoology*, **38**, 7–25.

Lewis, P.O. (2001) A likelihood approach to estimating phylogeny from discrete morphological character data. *Systematic Biology*, **50**, 913–925.

Lioy, P. (1864) I ditteri distribuiti secondo un nuovo metodo di classificazione naturale (Syrphidi). *Atti dell'Imperiale Regio Istituto Veneto di Scienze, Lettere ed Arti (3)*, **9**, 738–760.

McAlpine, J.F. (1981) Morphology and terminology – Adults. *Manual of Nearctic Diptera*, **1**, 9–63.

Mengual, X., Ståhls, G. & Rojo, S. (2008) First phylogeny of predatory flower flies (Diptera, Syrphidae, Syrphinae) using mitochondrial *COI* and nuclear *28S* rRNA genes: conflict and congruence with the current tribal classification. *Cladistics*, **24**, 543–562.

Metcalf, C.L. (1921) The genitalia of male Syrphidae: their morphology, with especial reference to its taxonomic significance. *Annals of the Entomological Society of America*, **14**, 169–228.

Mirande, J.M. (2009) Weighted parsimony phylogeny of the family Characidae (Teleostei: Characiformes). *Cladistics*, **25**, 574–613.

Papavero, N. (1962) Quatro novas espécies de Microdontinae do Brasil (Diptera, Syrphidae). *Papéis Avulsos do Departamento de Zoologia*, **15**, 317–326.

Rafael, J.A. & De Meyer, M. (1992) Generic classification of the family Pipunculidae (Diptera): a cladistic analysis. *Journal of Natural History*, **26**, 637–658.

Reemer, M. (2008) *Surimyia*, a new genus of Microdontinae, with notes on *Paragodon* Thompson, 1969 (Diptera, Syrphidae). *Zoölogische Mededelingen*, **82**, 177–188.

Reemer, M. & Ståhls, G. (2013) Generic revision and species classification of Microdontinae (Diptera: Syrphidae). *Zookeys*, **288**, 1–213.

Rondani, C. (1845) Ordinamento sistematico dei generi italiani degli insetti ditteri. *Nuovi Annali delle Scienze Naturali, Bologna* **1844**, **2**, 443–459.

Ronquist, F. & Huelsenbeck, J.P. (2003) MRBAYES 3: bayesian phylogenetic inference under mixed models. *Bioinformatics*, **19**, 1572–1574.

Ronquist, F., Huelsenbeck, J. & Tslenko, M. (2011) *Draft MrBayes Version 3.2 Manual: Tutorials and Model Summaries* [WWW document]. URL http://mrbayes.sourceforge.net/mb3.2_manual.pdf [accessed on 15 July 2012]

Rosenberg, M. (ed.), (2009) *Sequence Alignment. Methods, Models, Concepts, and Strategies*. University of California, Berkeley, CA.

Rotheray, G.E. & Gilbert, F.S. (2008) Phylogenetic relationships and the larval head of the lower Cyclorrhapha (Diptera). *Zoological Journal of the Linnean Society*, **153**, 287–323.

Sabrosky, C.W. (1999) Family-group names in Diptera. *Myia*, **10**, 1–576.

Sereno, P.C. (2007) Logical basis for morphological characters in phylogenies. *Cladistics*, **23**, 565–587.

Shannon, R.C. (1925) An extraordinary adult myrmecophile from Panama. *Proceedings of the National Academy of Sciences, U.S.A.*, **10**, 211–213.

Shatalkin, A.I. (1975a) A taxonomic analysis of the hoverflies (Diptera, Syrphidae). I. *Entomological Review*, **54**, 117–125.

Shatalkin, A.I. (1975b) A taxonomic analysis of the hoverflies (Diptera, Syrphidae). II. *Entomological Review*, **54**, 127–134.

Sinclair, B.J. (2000) Morphology and terminology of Diptera male terminalia. *Contributions to a Manual of Palaearctic Diptera*, **1**, 53–74.

Skevington, J.H. & Yeates, D.K. (2000) Phylogeny of Syrphoidea (Diptera) inferred from mtDNA sequences and morphology with particular reference to classification of the Pipunculidae (Diptera). *Molecular Phylogenetics and Evolution*, **16**, 212–224.

Speight, M.C.D. (1987) External morphology of adult Syrphidae (Diptera). *Tijdschrift voor Entomologie*, **130**, 141–175.

Speight, M.C.D. (2010) Species accounts of European Syrphidae (Diptera) 2010. *Syrph the Net, the Database of European Syrphidae*, Vol. **59**, pp. 1–285. Syrph the Net Publications, Dublin.

Ståhls, G., Hippa, H., Rotheray, G., Muona, J. & Gilbert, F. (2003) Phylogeny of Syrphidae (Diptera) inferred from combined analysis of molecular and morphological characters. *Systematic Entomology*, **28**, 433–450.

Steyskal, G.C. (1953) A new melissomimetic fly of the genus *Microdon* (Diptera, Syrphidae). *Occasional Papers of the Museum of Zoology, University of Michigan*, **551**, 1–4.

Thompson, F.C. (1969) A new genus of Microdontine flies (Diptera: Syrphidae) with notes on the placement of the subfamily. *Psyche*, **76**, 74–85.

Thompson, F.C. (1972) A contribution to a generic revision of the Neotropical Milesinae (Diptera: Syrphidae). *Arquivos de Zoologia*, **23**, 73–215.

Thompson, F.C. (1974) The genus *Spheginobaccha* de Meijere (Diptera: Syrphidae). *Transactions of the American Entomological Society*, **100**, 255–287.

Thompson, F.C. (1981) Revisionary notes on Nearctic *Microdon* flies (Diptera: Syrphidae). *Proceedings of the Entomological Society of Washington*, **83**, 725–758.

Thompson, F.C. (1999) A key to the genera of the flower flies (Diptera: Syrphidae) of the Neotropical region including descriptions of new genera and species and a glossary of taxonomic terms. *Contributions on Entomology, International*, **3**, 321–378.

Thompson, F.C., Vockeroth, J.R. & Sedman, Y.S. (1976) Family Syrphidae. *A Catalogue of the Diptera of the Americas South of the United States*, **46**, 1–195.

Verrall, G.H. (1901) Platypezidae, Pipunculidae and Syrphidae of Great Britain. *British Flies*, **8**, 1–691.

Vockeroth, J.R. & Thompson, F.C. (1987) Syrphidae. *Manual of Nearctic Diptera*, **2**, 713–743.

Williston, S.W. (1886) Synopsis of the North American Syrphidae. *Bulletin of the United States National Museum*, **31** i–xxx, 1–335.

Yeates, D.K., Wiegmann, B.M., Courtney, G.W., Meier, R., Lambkin, C. & Pape, T. (2007) Phylogeny and systematics of Diptera: two decades of progress and prospects. *Zootaxa*, **1668**, 565–590.

Accepted 10 April 2013
First published online 21 June 2013